University of Zawia

Faculty of Engineering

Electrical and Electronic Department

Power Engineering Section

Zawia - Libya

Brain tumor detection by multi focus image fusion based on wavelet transform

A Dissertation Submitted to the Faculty of Engineering, University of Zawya in Fulfillment of the Requirements for Degree of Master of Science in the Department of Electrical and Electronic Engineering

Presented By: ***Munira Habib Abdul Latif***

Supervised by: ***prof. Ali Al-Amouri***

Fall 2020

الإهـــــــــــداء

إلـــى مـــن علمنـــي إن دنيـــا كفـــاح ... وســـــــلاحها العلـــــم والمعرفـــــة

إلـــى الـــذي لـــم يبخـــل علـــي بـــأي شـــي ... إلـــى أعظـــم واعـــز رجـــل أبـــي الغـــالي

إلـــى مـــن ســـاندتني فـــي صـــلاتها ودعائهـــا ... إلـــى مـــن ســـهرت الليـــالي تنيـــر دربـــي

إلـــى مـــن تشـــاركني أفراحـــي وإحزانـــي ... إلى أجمل ابتسامه فـي حياتي أمـي الغالية

إلـــى الـــذين ظفـــرت بهـــم هديـــة أخـــواتي ... إلـــــى حبيبـــــاتي رغـــــد و رنـــــا

Acknowledgements

In the name of God, the Most Gracious, the Most Merciful. Praise be to God, Lord of the Universe, to give me the mercy to complete this project. I am grateful for the sincerity and heart of my supervision, prof. Ali Al-Amouri for the support and guidance he provided to me throughout the writing of my letter. I appreciate his positive comments and advice and all his direction, time and assistance while studying and preparing the project. A special thanks to Dr. Moftah Al-Murabit for his encouragement during my academic life and his support in pursuing my career and all the lecturers at The University Of Zawia for the wealth I gained from their lectures.

I take this opportunity to register my sincere thanks to Dr. Mustafa Al-Aswad, Dr. Faraj and all my friends for their help and encouragement.

I would like to thank my family members for their support.

ملخص

يعتبر ورم المخ أو السرطان من أخطر أنواع السرطانات لأنه يصيب الجهاز العصبي الرئيسي لجسم الإنسان ، كما أن الكشف عن أورام المخ مهمة معقدة وحساسة تدل على خبرة الطبيب. في هذه الدراسة تم اقتراح طريقة "اكتشاف ورم الدماغ عن طريق دمج الصورة متعدد التركيز بناءً على تحويل المويجات ".حيث تم دمج صور التصوير بالرنين المغناطيسي (MRI) والصور المقطعية (CT) من أجل تعزيز اكتشاف الورم .السبب الرئيسي لدمج صور متعددة التركيز هو مساعدة الأطباء في الحصول على دعم في التشخيص .تم تنفيذ الخوارزمية باستخدام سبع مويجات وهي: bior2.2 و coif2 و db2 و dmey و rbio2.2 و sym4 و haarعلى التوالي للحصول على مجموعة متنوعة من النتائج. تستخدم هذه الخوارزمية بشكل فعال المعلومات التي توفرها صور التصوير بالرنين المغناطيسي والصور المقطعية للحصول على صورة مدمجه ناتجه مما يزيد من كفاءة اكتشاف الورم باستخدام الماتلاب. تم تقييم فعالية الخوارزمية من خلال تغيير معاملات اندماج المويجات مثل عدد التحلل ومقياس جودة الصورة ; والمقياس الذي تم استخدامه لقياس جودة صوره هو حساب نسبة الإشارة إلى نسبة ضوضاء(PSNR) وحساب معامل العشوائية (Entropy Factor). وقد لوحظ أن موجات haar تعطي أفضل النتائج مع حساب نسبة الإشارة إلى نسبة ضوضاء(PSNR) وتعطي موجات dmay أفضل النتائج مع حساب معامل العشوائية (Entropy Factor) للكشف عن الورم. وتم أيضًا تطبيق خوارزمية تجزئة على الصورة المدمجة التي تم الحصول عليها لتحديد الجزء المصاب بالورم والإشارة إلى منطقة نموه ، وسيتم عرض النتائج ومناقشتها.

ABSTRACT

Brain tumor or cancer is one of the most dangerous types of cancer because it affects the main nervous system of the human body, and the detection of brain tumors is a complicated and sensitive task that implied the experience of the classifier.

This thesis has suggested method of "Brain tumor detection by multi focus image fusion based on wavelet transform" .It combined Magnetic Resonance Imaging(MRI) and Computed Tomography (CT) image in order to enhance the tumor detection. The reason to incorporate multi -focus image is to help clinicians obtain support in diagnosing. The algorithm based on seven wavelets has been implemented, bior2.2, coif2, db2, dmey, rbio2.2, sym4 and haar respectively to get a variety of results. This algorithm is effectively used the information provided by the CT image and MRI images to obtain a resultant fused image which increases the efficiency of tumor detection by using MATLAB. The effectiveness of the algorithm was evaluated by changing the wavelet fusion parameters such as the number of decompositions and image quality; The scale that was used to measure its image quality is to calculate the signal-to-noise ratio (PSNR) and the calculation of the factor of randomness (Factor Entropy). It has been observed that the haar waves give the best results with the calculation of the signal to noise ratio (PSNR) and the dmay waves give the best results with the calculation of the factor of randomness (Factor Entropy) to detect the tumor.

A segmentation algorithm was also applied to the combined image obtained to identify the part affected by the tumor and indicate its area of growth, and the results will be presented and discussed.

Acronyms

MRI … Magnetic Resonance Imaging

CT … Computed Tomography

DT … Dual Tree

CWT … Continuous Wavelet Transform

PET … Positron Emission Tomography

GA … Genetic Algorithm

PSNR … Peak Signal to Noise Ratio

DWT … Discrete Wavelet Transform

IDWT … Inverse Discrete Wavelet Transform

FIR … Finite Impulse Response

SPECT … Single Photon Emission Computed Tomography

TABLE OF CONTENTS

List of Figures

List of tables

CHAPTER ONE
INTRODUCTION

1.1General background

Brain tumor is the mass or growth of abnormal cells in the brain there are two main types of brain tumors[1]: (i) Benign Tumor: Benign tumor is a tumor where they are having their boundaries or the edges in which they does not spread over the other parts of the body. It is considerably serious if they are meant to be in the important areas of the brain. It can step in to the disability and even it lead to the death .(ii) Malignant Tumor: Malignant tumor is considered to be the most serious one and they develop rapidly. They affect the various necessary organs which even lead to the death. About 80% of the malignant tumors are referred to as the gliomas; it refers to the tumor which has been originating from the gilial cells of the brain [2]. Figure (1.1) shows damaged brain cells.

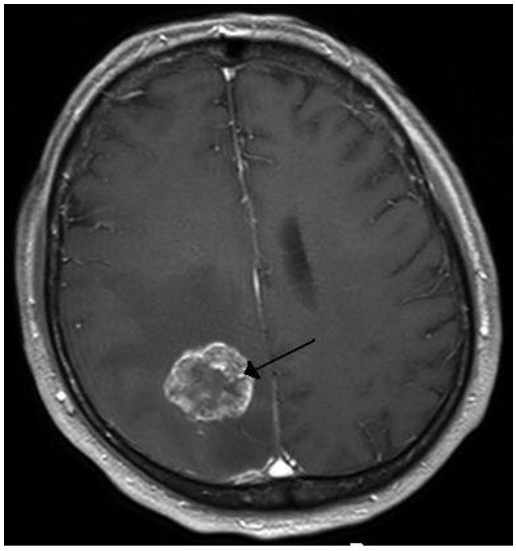

Fig(1.1) Brain Tumor

Magnetic Resonance Imaging (MRI) provides clear information about soft tissue and Computed Tomography (CT) gives bone structures [3] .Fusion is mechanism in which two or more input images are united to obtain new image as a fused image. Fused image have more accurate and relevant information than the input images. Medical image fusion is significant in medical field to combine two or more human body images

into one [4]. It is very useful to identify diseases in human body and possible diagnosis so that good treatment applied, The objective of medical image fusion is to maximize the information and improve the quality of the image by collecting strongest features provided by different modalities.

1.2 literature review

The study of cancerous tumor has attracted the attention of many researchers around the world. Hundreds of researches are being published yearly that discuss issues related to the brain tumor and the different methods for its early detection. Some of these researches rely on the use of image processing techniques like segmentation in their proposed works. Others use artificial intelligence structure to perform such tasks. In other types of researches, a combination of different detection methods is being implemented to perform the detection. In [5], presented a comprehensive review of research and developments in Combining complex Magnetic Resonance Imaging (MRI)and Computed Tomography (CT)Complex Wavelets using Technique Dual-tree complex wavelet transform (DT-CWT). Images were combined using three types of shift invariant wavelet transform (SIDWT), Discrete Wavelet Transform(DWT) and DT-CWT technologies. The images in the study were compared by means of the quantitative scale, and it was proven that the merging process using (DT-CWT) provides improved qualitative and quantitative results compared to the other two methods. Furthermore [6], the images were analyzed by Wavelet Transform, for medical applications (MRI and CT) using MATLAB, and the images were analyzed by Wavelet Transform, The sub domains of both images were combined using Inverse Discrete Wavelet Transform (IDWT), The resulting combined image was good and contains a complementary image

for both images . But [7], A wavelet-based image merging algorithm has been applied to Magnetic Resonance Image (MRI) and Computerized Tomography (CT) images which are used as primary sources to extract redundant and complementary information in order to enhance tumor detection in the resulting combined image. To detect brain tumor, tumor location, and tumor size, combine images using different wavelet transform parameters. The algorithm tool was evaluated applied to the images with respect to various wavelets type used for the wavelet analysis. on the basis of PSNR values. The results were compared with the segmentation logarithm and the Greta Van Fleet (GVF) logarithm, and it became clear that the proposed method gives the best results for estimating the tumor area and the computational efficiency of the algorithm is better than other methods. In [8], A new approach to integrate medical images using discrete wavelet transduction and the algorithm was applied to the Positron Emission Tomography(PET) image. This image shows brain function but it has low spatial resolution, the MR image shows this type of brain tissue image. Using Matlab, each image was analyzed using DWT, and the parameter was combined using the rule of low and high band fusion, and the molten parameters were reconstructed using I DWT, and this algorithm gave better results than the classical fusion models such as IHS & PCA and the algorithm was evaluated by PSNR and RMSE . Furthermore [9], Detection of a detached wavelet-based brain tumor based on the HAAR algorithm has been proposed In The proposed technique that s data base image and another is the input image in which both are decomposed into several bands by using wavelet transform and their coefficients are stored into matrix form with the help of MATLAB and these coefficients are compared with the help of mutual information principle. High-frequency corrected sub bands and interpolated input image were combined with reverse DWT

(IDWT),a combined image of high quality was obtained to detect brain tumor, and also to detect breast cancer. But [10], the concepts related to image segmentation, basics of MRI, clinical applications of MRI and MRI of brain tumors are described The further presented a novel algorithm for segmentation and classification of brain tumors. The thresholding approach is used for image segmentation which helps to recognize the portion of tumor in MR image. Then using the approach of Discrete wavelet transform (DWT) and Principal Component Analysis (PCA) for feature extraction and reduction, the texture features like contrast, correlation, energy along with the statistical features like mean, variance, skewness, smoothness, kurtosis, standard deviation and entropy are extracted using the gray level co-occurrence matrix. Using this algorithm the brain tumors are accurately segmented. In [11], of combining different data from two unique methods was performed to build prescriptive ability. In this work, an image set based on a Genetic Algorithm (GA) was performed with the help of continuous medical images. A genetic algorithm is an evolutionary procedure. For the combination, using two important GA officials called hybrid and change. The proposed system was implemented in two versions of Magnetic Resonance Imaging (MRI) and Computed Tomography (CT), The implementation of the proposed system was evaluated with various quality measures . Furthermore [12], presented dealted with the idea is to improve the image content by fusing images like Computer Tomography (CT) and Magnetic Resonance Imaging (MRI) images, so as to provide more information to the doctor and clinical treatment planning system. This stady based on the wavelet transformation to fused the medical images. The wavelet based fusion algorithms used on medical images CT and MRI, This involve the fusion with MIN , MAX, MEAN method. This fusion algorithm, is an effective approach in image fusion

area . In this thesis an approach for brain tumor detection by multi focus image fusion using wavelet transform like bior2.2, coif2, db2, dmey, rbio2.2, sym4 and haar .And the result obtained will be compared.

1.3 Problem Statement

- This study deals with the selection of wavelet function, and the use of wavelet-based fusion algorithms in integrating medical images of CT scans and MRIs, implementing fusion rules and assessing fusion image quality by calculating the efficiency of the resulting image using the PSNR and Entropy factor**.**
- This study deals with the is the detection of the brain tumor for efficient cure of the patients.

1.4 Methodology

In order to achieve the goals of this work and meet the requirements for participation in solving the proposed problem, this work will be arranged in the order that provides the best results and will be prepared within the capabilities of the message. First of all, data will be collected from different MR images and CT images of the brain. Due to lack of database resources for brain tumor images, the database will be merged from different sources. In this study, A method has been suggested for detection brain tumor by merging multi-focus images using discrete wavelet transform Discrete Wavelet Transform (DWT) and Inverse Discrete Wavelet Transform (IDWT).The MRI and CT images are merged by taking the absolute maximum of the wavelet coefficients with more brightness and maintains the prominent features of each . Image merging is the process of selecting useful and accurate information from individual source images. It is important to maintain the quality of the source images. Quality Preservation plays a major role in image merging technology. In this study, will improve the source images before

merging ,but to improve the source images will use wavelet transformation.

1.5 Objective of this Research

The objectives of the thesis can be summarized as follows:

- The multi -focus imaging is used to present an integrated image of the human brain.
- Support the physicians who need to fusion multi-modality images for diagnosis.
- Improve medical images by combining CT and MRI images, and choosing the best wavelet for that.

1.6 Thesis Organization

This thesis is divided into five chapters.

Chapter one:

The first chapter includes a basic introduction and a literary review of the project and gives a comprehensive overview of the thesis .

Chapter Two:

This chapter discusses the introduction to wavelets and the theory of discrete wavelet transformation.

Chapter three :

The third chapter discusses the background for image fusion based on wavelet transform, and the process of segmentation and methods of measuring the quality of the images.

Chapter Four :

In the fourth chapter the algorithm was applied to the data using MATLAB and results were compared in the first and second decomposition levels.

Chapter Five:

This chapter provides the results of this thesis, the conclusion of the proposed method , and also provides some recommendations for future work.

CHAPTER TWO
Wavelets

2.1 Introduction

The Wavelet series is just a sampling version of the CWT and its calculation can consume a significant amount of time and the resources that depend on the resolution required for the signal. DWT relies on sub band encoding resulting in a quick calculation of easily performed wavelet transformation, DWT dates back to 1976 when technologies were developed to separate time signals that resemble the work done in encoding a voice signal called sub domain encoding. In 1983, a similar technology for coding sub domains was called hierarchical coding. Subsequently, various enhancements were made to these coding schemes resulting in efficient multiple precision analysis schemes. Signals are analyzed using a set of basic functions that relate to simple scale and translation, containing only the scale function and the translation function. In this case of the DWT we obtain an image scale representation of the digital signal obtained using digital filtering techniques. DWT is applied to the image and it is a very simple procedure in which we assume that the image contains ω (j + 1. m. n) because j + 1 is the scale function m is the row vector and n is the column vector. Applies to the high pass filter hψ (-n) and also to the low pass filter h (-n). The filter is applied through the column where n denotes the column and either divides the overall signal into two filters like a low pass filter and a high pass filter[9].

2.2 Wavelet families

Wavelet transform is used to suppress the noise which is out of frequency band of the signal There are various types of wavelet among which Haar wavelet is the simplest technique ,Haar transform is mathematical operation applied on Haar wavelets. Due to its simplicity Haar transform can be taken as reference for all other wavelet transforms.

The Haar transform is based on decomposition principle where a discrete signal is broken into two sub signals of each half of original length. Average running subsignal is known as trend and the difference running sub signal is known as fluctuation. Haar transform is simple and low cost and easy to apply. Limitation of Haar wavelet transform technique is its inability in providing compression and noise removal for audio signal processing applications. The Daubechies wavelet is an alternative to Haar wavelet but faces with limitations of its complexity and cost.. The other type of wavelet is Symlets which are a modified version of Daubechies wavelets. It increases the symmetry[13].

2.2.1 Haar Wavelet

The Haar wavelet is a sequence of rescaled "square-shaped" functions which together form a wavelet family or basis. It allows a target function over an interval to be represented in terms of an orthonormal function basis [14]. Since it is not continuous in nature, it cannot be differentiable. Wavelet function$\varphi(t)$ and scaling function$\emptyset(t)$ of the Haar wavelet is represented as[15]:

$$\varphi(t) = \begin{cases} 1 & 0 \leq t < 1/2 \\ -1 & 1/2 \leq t < 1 \\ 0 & \text{otherwise} \end{cases} \qquad (2.1)$$

$$\emptyset(t) = \begin{cases} 1 & 0 \leq t < 1 \\ 0 & \text{otherwise} \end{cases} \qquad (2.2)$$

Figure(2.1) shows the wavelet function of haar in which x-axis represents the time and y-axis represents the frequency.

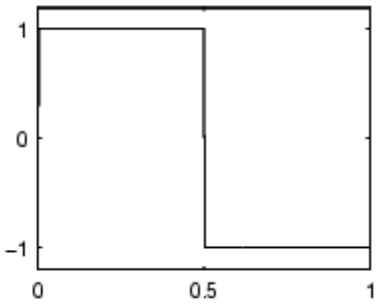

Fig(2.1) Wavelet function of Haar

2.2.2 Daubechies wavelet

Discover Ingrid Daubechies wavelet. Daubechies wavelets are compression supported orthogonal wavelets[16]. These are popular wavelet filters with certain limits, these filters can produce perfect reconstruction. The Daubechies wavelet is made up of different types of wavelets, Daubechies family wavelets are written dbN, where N is the order, and db the "surname" of the wavelet. The db1 wavelet, as mentioned above, is the same as Haar wavelet[17]. Figure (2.2) shows the wavelet function of daubechies in which x-axis represents the time and y-axis represents the frequency.

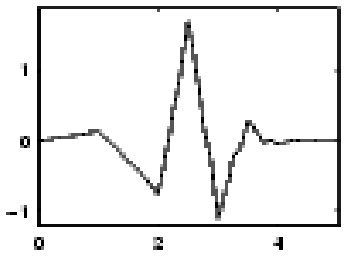

Fig(2.2) Wavelet function of Daubechies

2.2.3Coiflets wavelet

The Coiflets were built by Ingrid Daubechies at the request of Ronald Coifman ,Coiflets wavelets are discrete in nature which contains the scaling function with number of vanishing moments. The wavelet belongs to the orthogonal wavelet family. For efficient implementation, these filters are compression compatible versus limited pulse response

filters. For both Wave size and functions These waves have a large number of fading moments when compressed. There are 2N moments of zero wavelength and 2N-1 moments of zero [17].

Figure (2.3) shows the wavelet function of coiflet in which x-axis represents the time and y-axis represents the frequency.

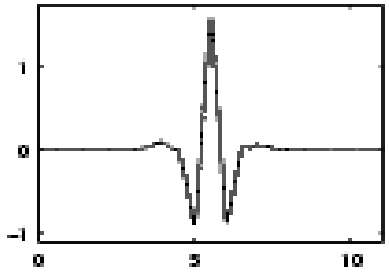

Fig(2.3) Wavelet function of coif2

2.2.4 Discrete Meyer (dmey) Wavelet

The discrete form of Meyer wavelet function is called dmey wavelet. These wavelets are symmetric and continuous with compact support. The basis function is biorthogonal[18]. Figure (2.4) shows the wavelet function of meyer in which x-axis represents the time and y-axis represents the frequency.

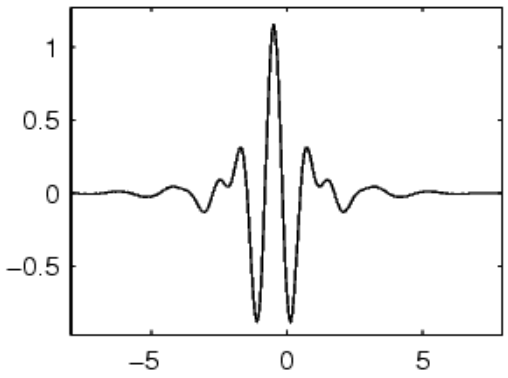

Fig(2.4)Wavelet function of meyer

2.2.5 Symlet (sym) Wavelet

have also been invented by Ingrid Daubechies. Symlets are more symmetric than Daubechies wavelets[19]. The wavelets are denoted as symN and have the same property as dbN. Symlet Wavelet is defined for any positive integer n. The scaling function and wavelet function have compact support length of 2n. Symlet Wavelet can be used with such functions as discreet wavelet transform [18].

Figure (2.5) shows the wavelet function of symlet in which x-axis represents the time and y-axis represents the frequency.

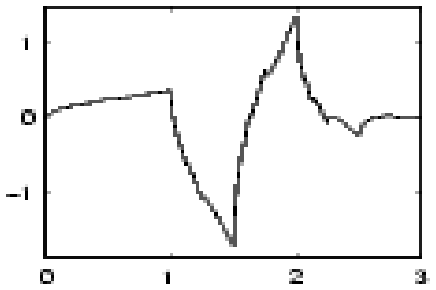

Fig (2.5)Wavelet function of Sym2

2.2.6 Biorthogonal (bior) Wavelet

A biorthogonal wavelet is one where the wavelet function is invertible and not necessarily orthogonal. this wavelet function increases flexibility and provides more degree of freedom Also, this supports the construction of symmetric wavelet function[18].

2.2.7 Reverse Biorthogonal (rbio) Wavelet

The reverse biorthogonal wavelet is the opposite of biorthogonal wavelet. The properties, scaling and wavelet functions remain the same but vary in the component selection for the fusion process[18].

2.3Wavelet transforms

Wavelet means small wave so wavelet analysis is about analyzing signal with short duration finite energy functions. They transform the

signal under investigation in to another representation [20]. wavelets have found a wide range of application in the field of signal processing such as image reconstruction and noise reduction. Wavelet conversion can be applied to digital images to provide some analysis tools and extract some kind of features. The idea of converting an image is implemented by transforming the image with respect to some features. Features are chosen in a way that ensures that effective pixel values are uncorrelated, in other words; Expressing the image in a compressed copy of it. Waves are functions that are created from mother function. This unique function is called the mother wavelet. Waves are created by measuring and translating the time or frequency field of the main function[21]. If the mother function is given by ψ (*t*), the other wavelets ψ*a,b*(*t*) can be given by [22]:

$$\psi_{a,b}(t) = \frac{1}{\sqrt{a}}\psi\left(\frac{t-b}{|a|}\right) \qquad (2.3)$$

where a and b are scaling and shifting parameters, respectively.

The wavelet transform of a function F(t) is defined as [22]:

$$W(a,b)=\int_t f(t)\frac{1`}{\sqrt{a}}\psi\left(\frac{t-b}{|a|}\right) \qquad (2.4)$$

According to equation(2.4), for every (a, b), we have a wavelet transform co-efficient, representing how much the scaled wavelet is similar to the function at location, t = b/a

There are two main groups of transforms, continuous and discrete wavelet transforms (DWT), Continuous wavelet transforms (CWT) and multi resolution based wavelet transform.

2.4 Discrete wavelet transforms (DWT)

The discrete wavelet transform is a spatial frequency domain disintegration that presents a bendable multi-resolution analysis of an

image [23]. which applies a two- channel filter bank (with down sampling) iteratively to the low pass band (initially the original signal). The wavelet representation then consists of the low-Analysis of CT and MRI Image Fusion using Wavelet Transform 2pass band at the lowest resolution and the high-pass bands obtained at each step. This transform is invertible and non redundant. The DWT is a spatial-frequency decomposition that provides a flexible multiresolution analysis of an image. the basic idea of the DWT is to represent the signal as a superposition of wave lets. Suppose that a discrete signal is represented by f (t); the wavelet decomposition is then defined as [24]:

$$f\ (\mathbf{t}) = \sum_{m,n} \boldsymbol{c}_{m,n}\ \psi_{\mathbf{m.n}}(\mathbf{t}) \qquad (2.5)$$

Where $\psi_{\mathbf{m.n}}(\mathbf{t}) = 2^{\frac{-m}{2}}\psi[2^{-m}t - n]$and m and n are integers. There exist very special choices of ψ such that $\psi_{m,n}$(t)constitutes an orthogonal basis, so that the wavelet transform coefficients can be obtained by an inner calculation:

$$C_{m,n} = \left(f\ ,\ \psi_{m,n}\right) = \int\ \psi_{m,n}(t)\, f(t)dt \qquad (2.6)$$

In order to develop a multiresolution analysis, a scaling function is φ needed, together with the dilated and translated version of it,

$$\varphi_{m,n}(t) = 2^{-\frac{m}{2}}\ \varphi[2^{-m}\ t - n] \qquad (2.7)$$

According to the characteristics of the scale spaces spanned by $\varphi$and ψ ,the signal *f (t)* can be decomposed in its coarse part and details of various sizes by projecting it onto the corresponding spaces. Therefore, to find such decomposition explicitly, additional coefficients $a_{m,n}$ are required at each scale. At each scale $a_{m,n}$ and a_m-1,$_n$ describe the approximations of the function *f (t)* at resolution $2^m$and at the coarser resolution 2^{m-1}, respectively, while the coefficient $C_{m,n}$ and describe the information loss when going from one approximation to another. In order

to obtain $a_{m,n}$ at each scale and position. The approximation coefficients and the wavelet coefficients can be obtained[24]:

$$a_{m,n}=\sum_k h\ 2^{(2-k)} a_{m-1,k} \quad (2.8)$$

$$C_{m,n} = \sum_k g\ 2^{(2-k)} a_{m-1,k} \quad (2.9)$$

Where, h_n is a low pass FIR filter and $g_n$is related high pass FIR filter. To reconstruct the original signal the analysis filters can be selected from a biorthogonal set which have a related set of synthesis filters. These synthesis filters $\tilde{h}$ and $\tilde{g}$ can be used to perfectly reconstruct the signal using the reconstruction[24] :

$$a_{m-1,l}(f) = \sum_n[\ \tilde{h}\ 2^{(2-l)} a_{m-n}\ (f) + \tilde{g}\ 2^{(2-l)} a_{m-n}(f)] \quad (2.10)$$

Equations (2.8) and (2.9) are implemented by filtering and down sampling. Conversely eqn.

(2.10) is implemented by an initial up sampling and a subsequent filtering .

2.4.1 Filter bank

Filter bank contains an association of filters. The constituent banks are synthesis bank and

analysis bank. Such filter banks are best suited with two channels. Figure (2.6) depicts the filter

bank architecture

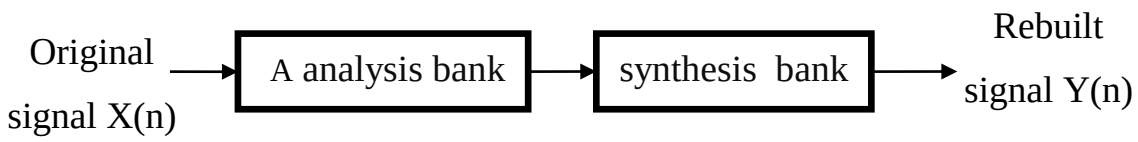

Fig(2.6) Filter bank

2.4.1.1 Analysis bank

There are two filters in the analysis bank:(a) One low pass filter,(b) One high pass filter.

These filters operate on input signal and separate them into their frequency bands. It is depicted in Figure (2.7). At the point when the signal navigates through these filters, the signal breaks down into four frequency bands, namely HH, HL, LH and LL. This process is called as 1st level of decomposition. It illustrates the detailed set of signal coefficients [25].

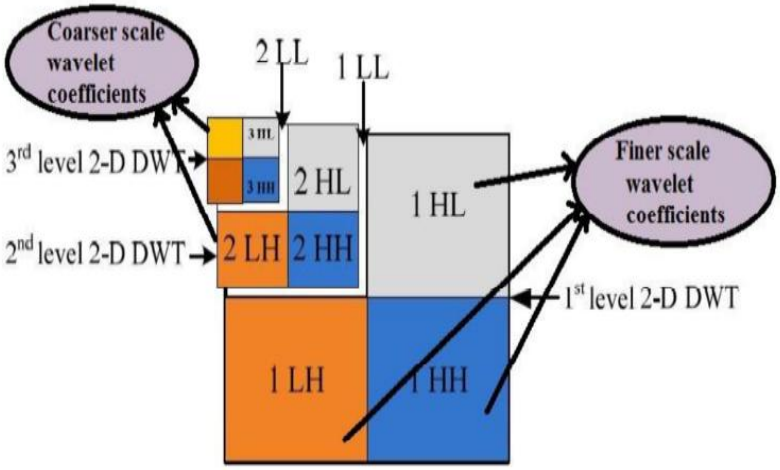

Fig (2.7) Wavelet coefficients with coarser scale and finer scale

The DWT uses wavelets, which are exploited to represent an image as an additive function involving such wavelets. These wavelets contain individual scale and location. The data will be represented into a set of low pass signals, known as approximate coefficients, and another set of high pass signals, known as detail coefficients. the data will be given as inputs to an array of high pass and low pass filters. The resulting outcomes of low pass filters and high pass filters will be down-sampled to a factor of 2 in the next step. Then again, the output of the high pass filter becomes the detail coefficient, and the output of low pass filter becomes the approximate coefficient. The process is illustrated in figure (2.8) which depicts the working of 1D DWT.

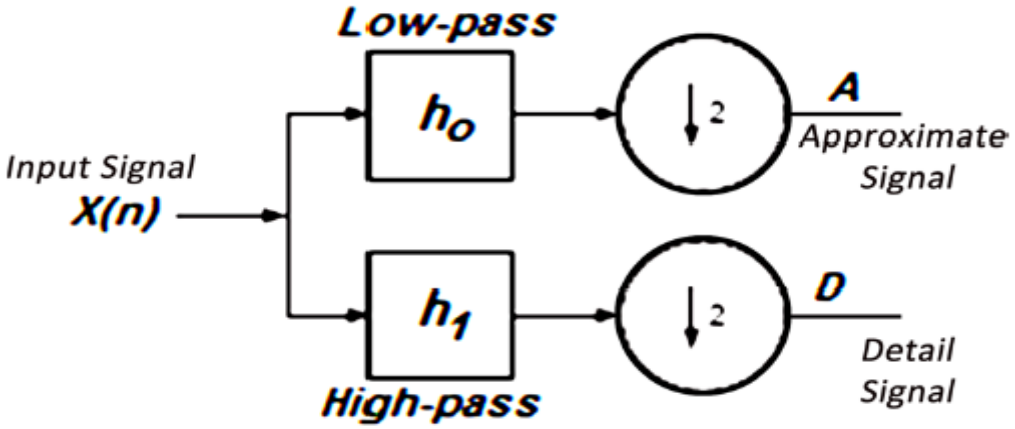

Fig(2.8) 1D DWT of Discrete wavelet transform

To achieve 2D DWT, the horizontal rows and vertical columns of given input signal is fed into both high pass and low pass filter, in mutual directions. Then the resulting sequence is sampled by a factor of 2 for both directions .The process is illustrated in figure (2.9) which depicts the working of 2D DWT.

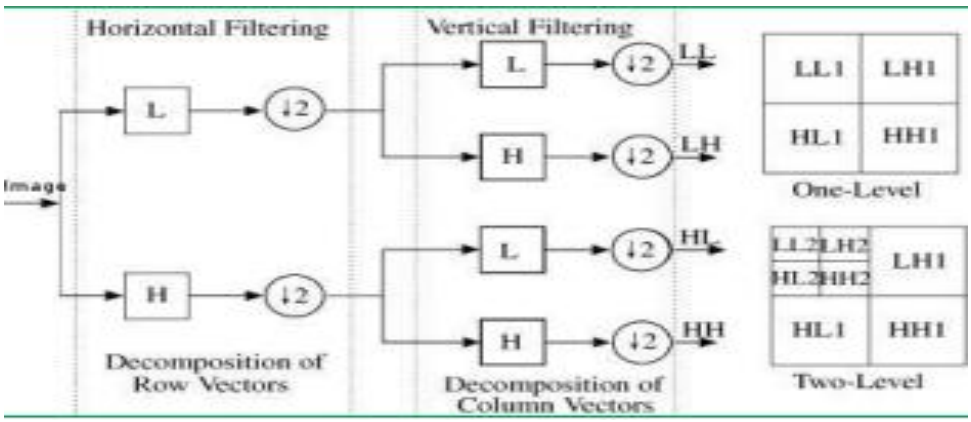

Fig(2.9) 2D of Discrete wavelet transform

2.4.1.2 Synthesis bank

Synthesis bank is the inverse operation of analysis bank. The synthesis bank in digital signal processing is composed of decimation and filtering the block diagram of synthesis bank is depicted in Figure(2.10). The wavelet coefficients and scaling coefficients of approximation signal can be combined to generate signal reconstruction of detail signal coefficients. Any image in 2 dimension is composed of horizontal rows

and vertical columns. The subsequent image decomposition results in wavelets involves which includes a pair of waveforms[25].

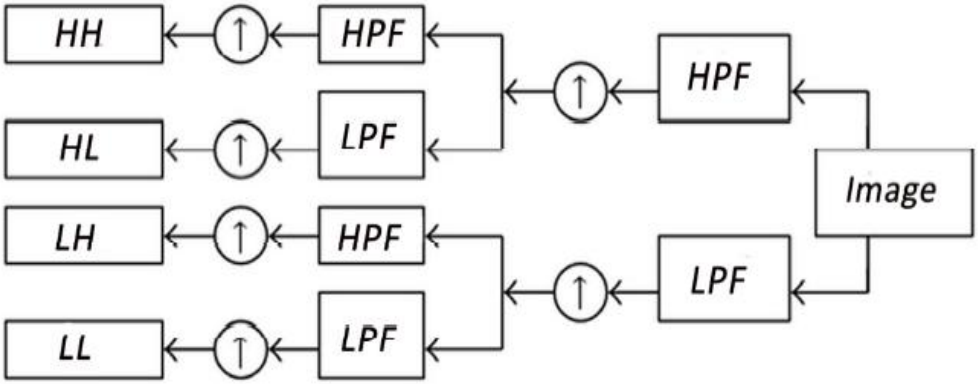

Fig(2.10)Inverse discrete wavelet transform of 2D

CHAPTER THREE

Image Fusion Based on Wavelet Transforms

3.1 Introduction

The wavelet transform is a mathematical tool that can detect local features in the signaling process. It can also be used to analyze one dimensional (1D) and two dimensional (2D) signals such as 2D grayscale image signals to different resolution levels to analyze multiple solutions Wavelet transformation has been used extensively in many fields, such as texture analysis, data compression, and feature detection And fusion of the image[24]..The most common form of transform type image fusion algorithms is the wavelet fusion algorithm due to its simplicity and its ability to preserve the time and frequency details of the images to be fused[26].

3.2 Image fusion

Image Fusion is used to retrieve important data from a set of images entered and put it in one output image to make it more informative and useful than any of the images entered. Improves data quality and application. The quality of the merged image depends on the application. Image integration is widely used in smart robots, stereo camera integration, medical imaging, manufacturing process monitoring. Using fusion two images can be merged to produce a single high resolution multispectral image. In medical applications, Image fusion is commonly used term. Medical images from the same modality or multiple modalities such as CT, MRI can be merged using fusion to generate a more informative image which can help in diagnosis and treatment[27].The fused image should have much more complete information which is more useful for human or machine perception[28]. Image fusion method can be generally grouped in to three categories Pixel level, feature level and decision level Pixel level fusion has the advantage that the images used contain the original measured quantities ,

and the algorithms are computationally efficient and easy to implement, the most image fusion applications employ pixel level based methods. Figure (3.1) shows the division of the image merging process into three categories.

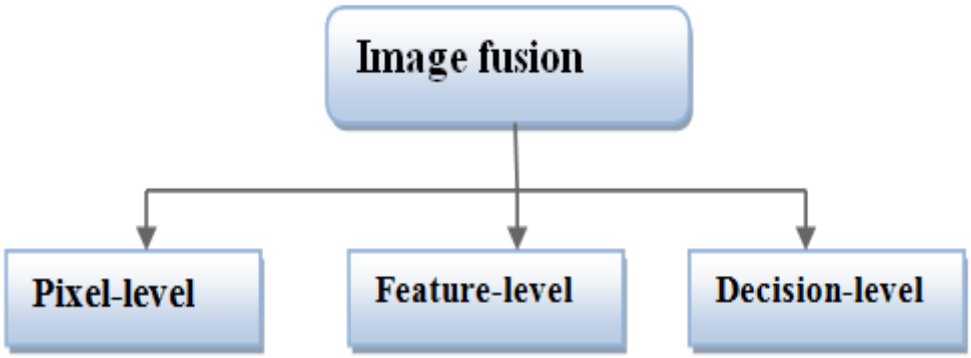

Fig(3.1) Image fusion categorization

- **Pixel-level:** It produces a fused image in which information content related with each pixel is concluded from a set of pixels in source images. Fusion at this level can be carry out either in spatial or in frequency domain. However, pixel level fusion may conduct to contrast reduction[23].
- **Feature-level:** In feature level process, features are extracted from input images .Image is segmented in continuous regions and fuse them using fusion rule. Features of images are combined such as size, shape, contrast, pixel intensities, edge and texture[29].
- **Decision-level:** Decision level is a superior level of fusion. Input images are processed independently for information mining, The obtained information is then united applying decision rules to emphasize widespread interpretation [23].

There are many rules for merging pictures, and they are as follows:

3.2.1 Select Maximum

In this method, the resultant fused image is obtained by selecting the maximum intensity of corresponding pixels from both input image[29]:

$$F(x,y)= \sum_{x=0}^{m} \sum_{y=0}^{n} \max\big(A(X,Y) + B(X,Y)\big) \quad (3.1)$$

Where A (x, y), B (x, y) are input image and F (x, y) is fused image. And point (x,y) is the pixel value

3.2.2 Select Average

In this method the resultant fused image is obtained by taking the average intensity of corresponding pixels from both input image[26]:

$$f(x,y) = \frac{(A(x,y)+B(x,y))}{2} \quad (3.2)$$

Where A (x, y), B (x, y) are input image and F (x, y) is fused image. And point (x, y) is the pixel value.

3.2.3 Select minimum

In this method, the resultant fused image is obtained by selecting the minimum intensity of corresponding pixels from both the input image[26]:

$$F(x,y)= \sum_{x=0}^{m} \sum_{y=0}^{n} \min\big(A(X,Y) + B(X,Y)\big) \quad (3.3)$$

Where A (x, y), B (x, y) are input image and F (x, y) is fused image. And point (x,y) is the pixel value.

Input images are processed individually for information extraction. The obtained information is then combined applying decision rules to reinforce common interpretation.

Based on domain, image fusion methods can be categorized into two domains [29]:

• spatial domain:

Spatial domain deals directly with pixel to integrate relevant information. Some of the spatial domain techniques include Averaging, select maximum/minimum method, Bovey transforms, Intensity Hue Saturation method (IHS), High Pass Filtering method (HPF), Principal Component Analysis method (PCA). Drawbacks of Spatial domain fusion include spatial distortion in new fused image. This spatial distortion problem is solved in frequency domain.

• frequency domain:

In frequency domain, image is transformed in frequency domain and frequency coefficients are combined to get fused image. Some of the transform domain fusion techniques include discrete wavelet transform, stationary wavelet transform.

Based on the input data and the purpose image fusion methods are classified as[29]:

• Multi-view fusion

Multi-view fusion combines the images taken by a sensor from different view- points at the same time. Multi-view fusion provides an image with higher resolution and also recovers the 3 -D representation of a scene.

• Multi-temporal fusion

Multi-temporal fusion integrates several images taken at various interval time to detect changes among them or to produce accurate images of objects.

• Multi-focus fusion

It is impossible for the optical lens to capture all the objects at various focal lengths .Multi-focus image fusion integrates the images of various focal lengths from the imaging equipment into a single image of better quality.

• Multi-modal fusion

Multi-modal fusion refers to the combination of images from different sensors and is often referred as multi-sensor fusion which is widely used in applications like medical diagnosis, security, surveillance, etc.

3.3 Wavelet analysis

Wavelet analysis is an effective methodology that is able to detect aspects of data that are missed by other signal analysis techniques such as trends, stops, breaks in higher derivatives, and self-similarity. Additionally, wavelet analysis is able to compress or remove noise from a signal without noticeable degradation. So wavelet the analysis is of the utmost importance in the case of sensitive information, such as medical imaging [30]. The idea for the basic algorithm is to divide the input images MRI and CT into secondary decay decomposition images using the forward wave transformation in the first level as shown in Figure (3.2).

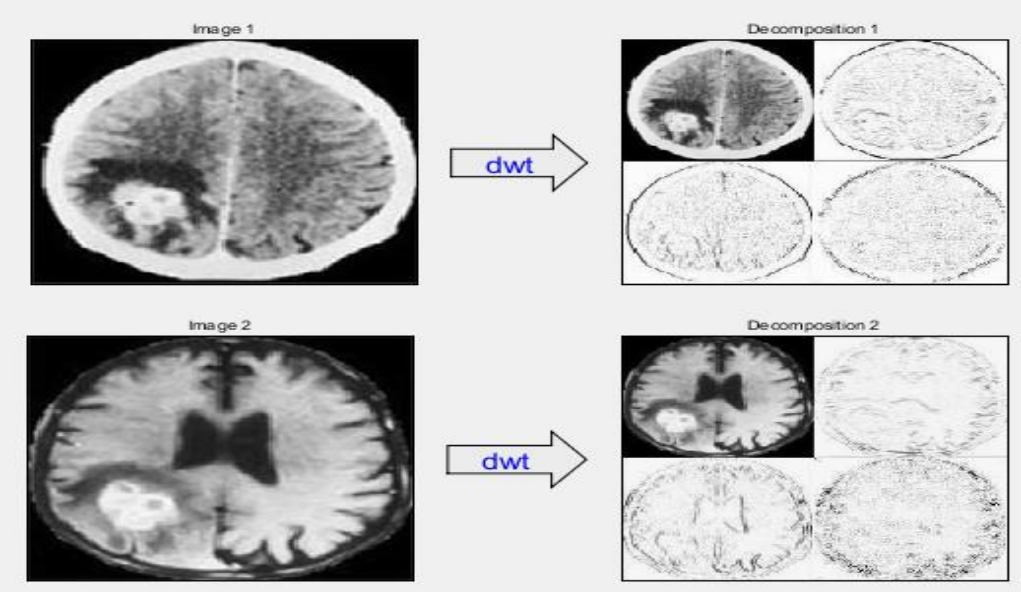

Fig(3.2) one level wavelet decomposition of CT and MRI image

As well as in dividing the input MRI and CT images into secondary decomposition images using forward wave conversion in the second level as shown in Figure (3.3)

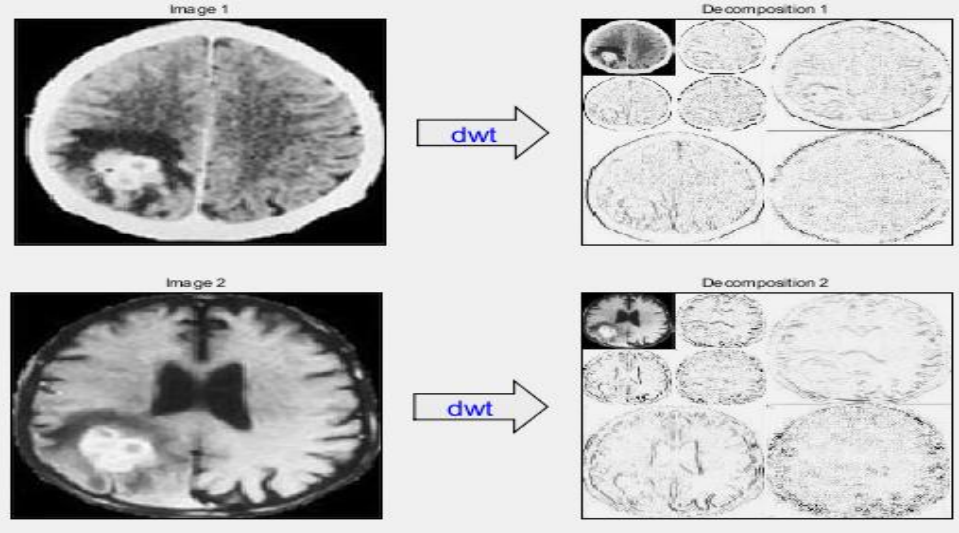

Fig (3.3)Two level wavelet decomposition of CT and MRI image

The source images such as CT and MR are decomposed in rows and columns by low-pass (L) and high-pass (H) filtering and subsequent down sampling at each level to get approximation Low-Low (LL) and detail Low-High (LH), High-Low (HL) and High-High (HH) coefficients. Scaling function is associated with smooth filters or low pass filters and wavelet function with high-pass filtering. Wavelet transforms provide a framework in which an image is decomposed, with each level corresponding to a coarser resolution band[6].

3.4 Wavelet Transform Fusion

The DWT is applied for both the source images and decomposition of each original image is achieved. This is embodied in the illustration of multiple scales where different bars (horizontal, vertical, diagonal and zero) represent a different parameter. There are two levels of decomposition, as shown in the upper left sub picture. The different black squares connected to each level of decomposition are associated with the

coefficient associated with the same spatial representation of the image in each original image that has the same pixel positions in the original image. Once a fused multi-scale is obtained, IDWT achieves the final fused image[31].

The Figure (3.4) illustrates the process of integrating images into a single plane of wavelet transformations.

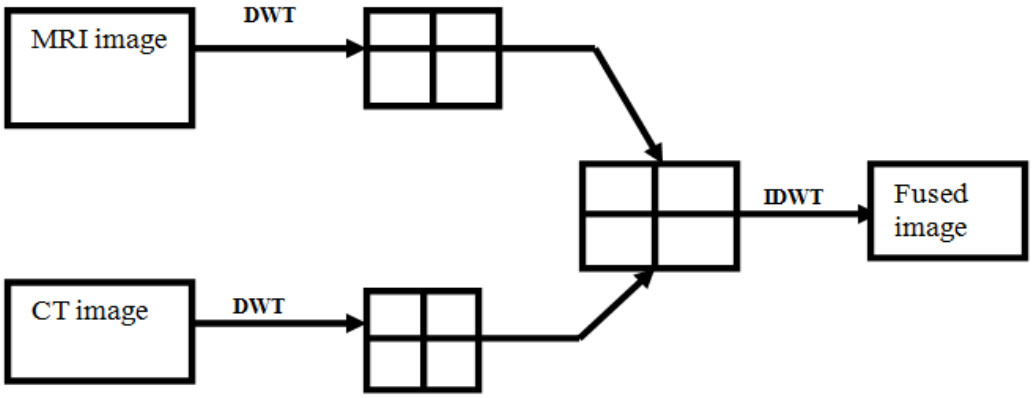

Fig (3. 4) Image merger diagram using one level wavelet transformations

Figure (3.5) illustrates the process of integrating images into the second level of wavelet transformations.

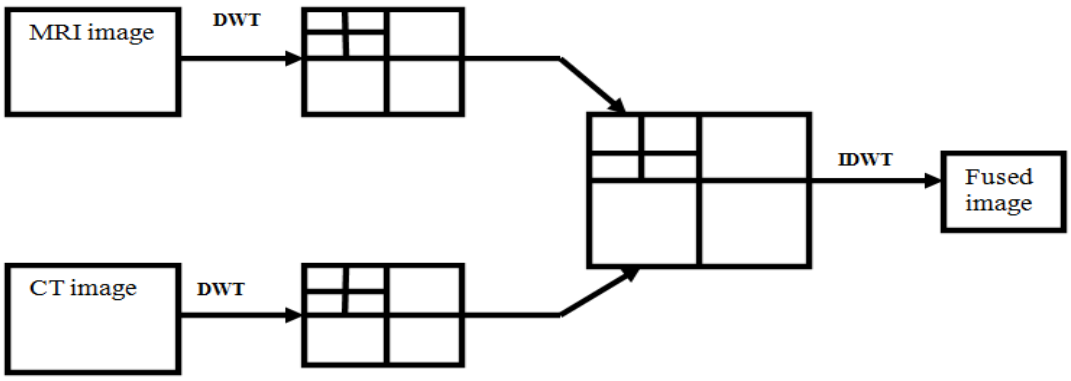

Fig(3.5) Image merger diagram using second level wavelet transformations

form of transformed image fusion is a wavelet transformation fusion it shares all the techniques of incorporating the field of conversion converted images it is merged into the transform field using a specific merge rule and then transformed again to the spatial domain to give the

resulting fused image. The wavelet transform fusion more officially determined by looking at the wavelet transformations ω from the recorded input images MRI I_1 (x, y) and CT I_2 (x, y) with the melting base φ. Then the reverse wavelet the conversion is calculated ω^{-1}, and the combined image I (x, y) is rebuilt[5]:

$$I(x, y) = \omega^{-1}\left(\varphi\left(\omega\left(I_1(x,y)\right), \omega\left(I_2(x,y)\right)\right)\right) \qquad (3.4)$$

3.5 Segmentation

Image segmentation is initial or front stage processing of image compression. The efficiency of segmentation process is its speed, good shape matching and better shape connectivity with its segmenting mainly focuses on identification of isolated points, lines and edges. In similarity based group those pixels which are similar in some sense, it includes approaches like thresholding, region growing, and region splitting and merging [32].

3.5.1 Segmentation by Thresholding

Thresholding methods are the simplest methods for image segmentation. These methods divide the image pixels with respect to their intensity level. These methods are used over images having lighter objects than background. The selection of these methods can be manual or automatic i.e. can be based on prior knowledge or information of image features by comparing all unallocated neighbouring pixels to the region. The difference between a pixel's intensity value and the region's mean is used as a measure of similarity.The pixel with the smallest difference measured is allocated to the respective region. This process stops when the intensity difference between region mean and new pixel become larger than a certain threshold (T). Finally output image is given

by combining both the regions. There are basically three types of thresholding [33][32].

3.5.1.1 Global Thresholding

This is done by using any appropriate threshold value/T. This value of T will be constant for whole image. On the basis of T the output image q(x ,y) can be obtained from original image p(x ,y)as[33]:

$$q(x,y)=\begin{cases}1, & \text{if } p(x,y) > T\\ 0, & \text{if } p(x,y) \le T\end{cases} \qquad (3.5)$$

3.5.1.2 Variable Thresholding

In this type of thresholding, the value of T can vary over the image. This can further be of two types[33]:

- Local Threshold: In this the value of T depends upon the neighborhood of x and y.
- Adaptive Threshold: The value of T is a function of x and y.

3.5.1.3 Multiple Thresholding:

In this type of thresholding, there are multiple threshold values like T0 and T1. By using these output image can be computed as[33]:

$$q(x,y) = \begin{cases}m, & \text{if } p(x,y) > T1\\ n, & \text{if } p(x,y) \le T2\\ 0, & \text{if } p(x,y) \le T0\end{cases} \qquad (3.6)$$

3.6 Quality Measurement

The measure of the efficiency or performance of the research method is a criterion for the improvement in the accuracy of the discrimination (details) of the image the result is visually, although the efficiency of the images from the merging process can be visually estimated there is still a need for digital scales. there are several measures to calculate the efficiency.

3.6.1 Coefficient of randomness (Entropy Factor)

Entropy indicates the amount of information contents present in the image. If the entropy is higher in the fused image then it indicates that fused image carrying greater information compare to the source image. The larger the value of entropy, better the fusion results.

The difference between the randomization coefficient of the two pictures was calculated, the resulting image from the fusion that is supposed to be high resolution, and the original image is of low resolution, as the difference in randomness indicates a degree the improvement in the accuracy of the discrimination, because the high values of the difference in randomness indicate that the percentage of improvement in the accuracy of the pictures high. The coefficient of randomness is a standard for measuring the amount of information in the resulting image, as it indicates density distribution and centralization of information within the field of the image. Entropy is a statistical measure of randomness that can be used to describe the texture of the input images and is represented by the equation[29].

$$\text{Entropy} = \sum f\left(log2\left(f(i,j)\right)\right) \quad (3.7)$$

3.6.2 Peak Signal to Noise Ratio (PSNR)

Peak Signal to Noise Ratio (PSNR) is an objective quality measurement of distortion. PSN Rcuses a constant value to compare the noise against the fluctuating signal used in Signal to Noise Ratio (SNR). Due to this reason the values received from the PSNR are treated more meaningfully when compared with different image coding algorithms [22]. The unit of PSNR is dB (decibel).

PSNR is defined as [22]:

$$\text{PSNR} = 20 * \log\left(\frac{256}{E}\right) \quad (3.8)$$

The root mean square error is given by Equation

$$E = \left[\frac{\sum_i (r_{i+d_i})^2}{mn}\right]^{\frac{1}{2}} \quad (3.9)$$

Where E is the root-mean-square-error, is the num-ber of pixels in the image, and r, d denotes the original and the fused image respectively.

CHAPTER FOUR
Experimental Results

4.1 Introduction

This chapter shows the results obtained in this thesis. All practical results of the logarithm application will be presented and discussed in this chapter. Different comparisons will be made under different criteria. Results will be scheduled, discussed and evaluated.

4.2 Implementation

Matlab R2016(9.0.0.341360) is used in the present study the patients images data obtained by MRI and computerized tomography are entered as an array of pixels in two dimensions of the matrix. the data are stored in Matlab .The images are displayed with grayscale or intensity levels. By default, these images can be determined by giving a large matrix whose entry points are between 0 and 255 and the process is done in several steps.

4.2.1 The first step

Image processing at this point is applied to source images (images MRI and CT)for different samples to increase contrast and brightness then the images are resized as 128*128 .

4.2.2 The second step

Wavelet transformation is applied to images MRI and CT separately by through different wavelet filters such as (haar , Daubechies ,,Coiflets... and others) in order to obtain the best performance.

4.2.3 The third step

The fusion technique of the MRI and CT images is obtained by taking the absolute maximum of the wavelet coefficients to get more brightness and maintaining the features of the two fused images and thus wavelet technologies can produce better results.

4.2.4 The fourth step

The merged wavelet image is reconstructed using inverse, obtaining a new merged image, and converted to binary format for ease of calculation and better efficiency to detect appropriate threshold values.

4.2.5 The Fifth step

The segmentation algorithm is applied to the wavelike fusion image, and the gray-plane image can be converted into a binary image. This algorithm is based on determining the threshold that gets the best result for detecting the tumor area as presented in the paper " Autmated brain tumor detection" is shown in the appendix [1], and the segmented image is represented by a two-dimensional matrix with values 0 and 1, all values of the gray level below the threshold will be classified as black 0, and values greater than the threshold are assigned white 1, Then small objects must be removed by setting a certain condition of pixel density in relation to the area of the object, the tumor is considered as the largest area object, and its location and area are detected to estimate the tumor boundaries in the fused image.

4.2.6 The six step

The performance of a reconstructed image is evaluated by using the parameters Peak Signal to Noise Ratio (PSNR) and Entropy Factor , different for wavelet decomposition in the first and second levels, and are compared. Figure (4.1) represents the flow chart of the proposed algorithm.

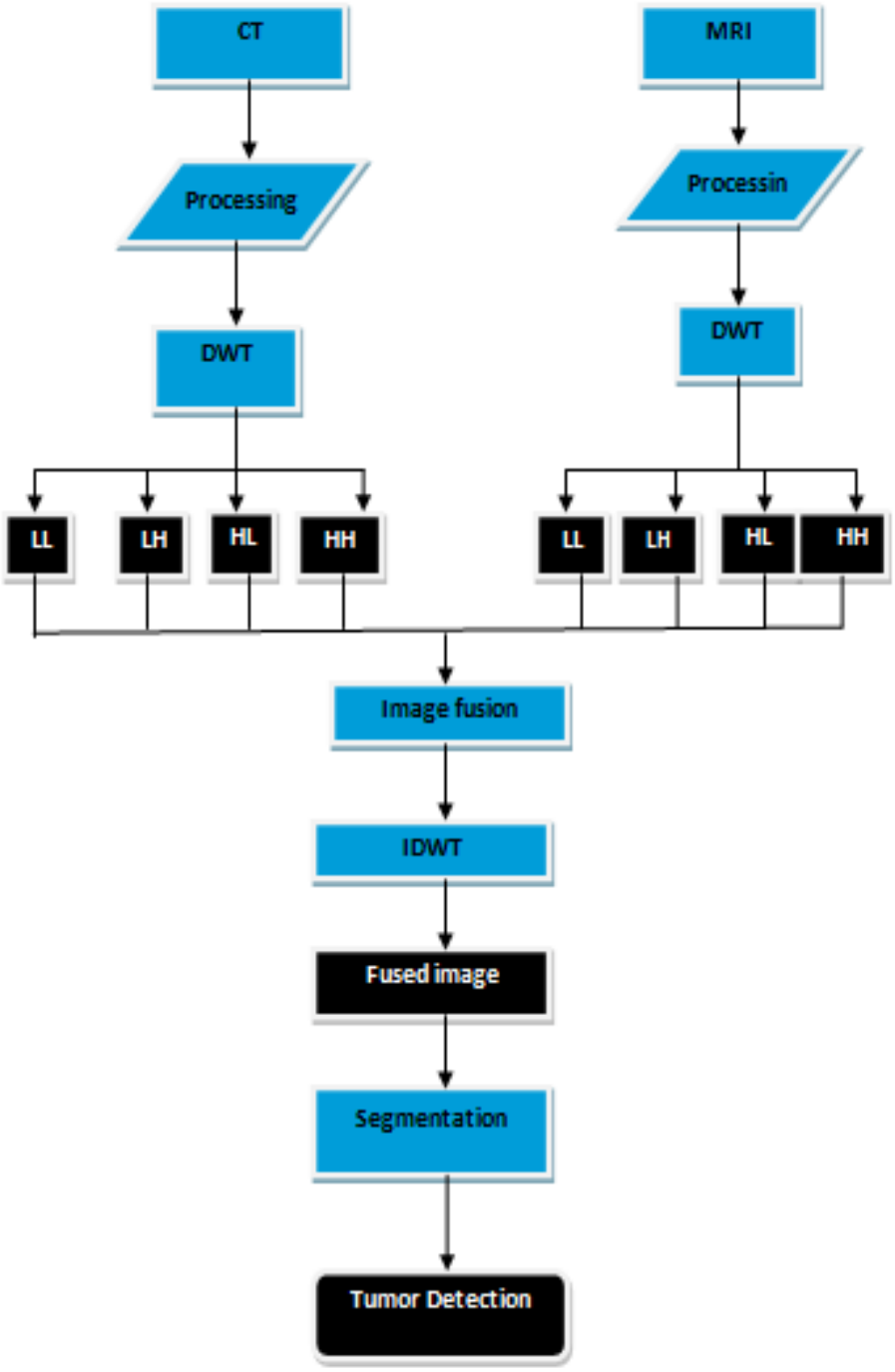

Fig (4.1) flow chart of the algorithm

4.3 Wavelet Fusion Algorithm

Choosing a reliable and efficient fusion method to determine the fusion coefficients is the key to image fusion. This study introduces a new algorithm and Discrete Waveform Operator (DWT) from the edge detection perspective. First analyze the original multimeter images with DWT, then obtain flat, vertical and diagonal edge information revealing the edges of low frequency and high frequency components. Next, perform a power-per-pixel comparison and check consistency to accurately identify edge points and ensure clarity of the blend image. The traditional method is compared with this new method from three aspects: independent factors, standardized factors and comprehensive evaluation. The experiment has demonstrated the usefulness of the method and is capable of preserving the edges and obtaining a better visual impact. with the variation of decomposition levels evaluate the performance of algorithm the errors are plotted with number of decompositions against the PSNR. The results are future illustrated by varying the wavelets for a given level of de-composition to give relative study. The performance of the various wavelets in order to obtain optimum results. The block diagram of the basic image fusion is shown in the figure (4.2).

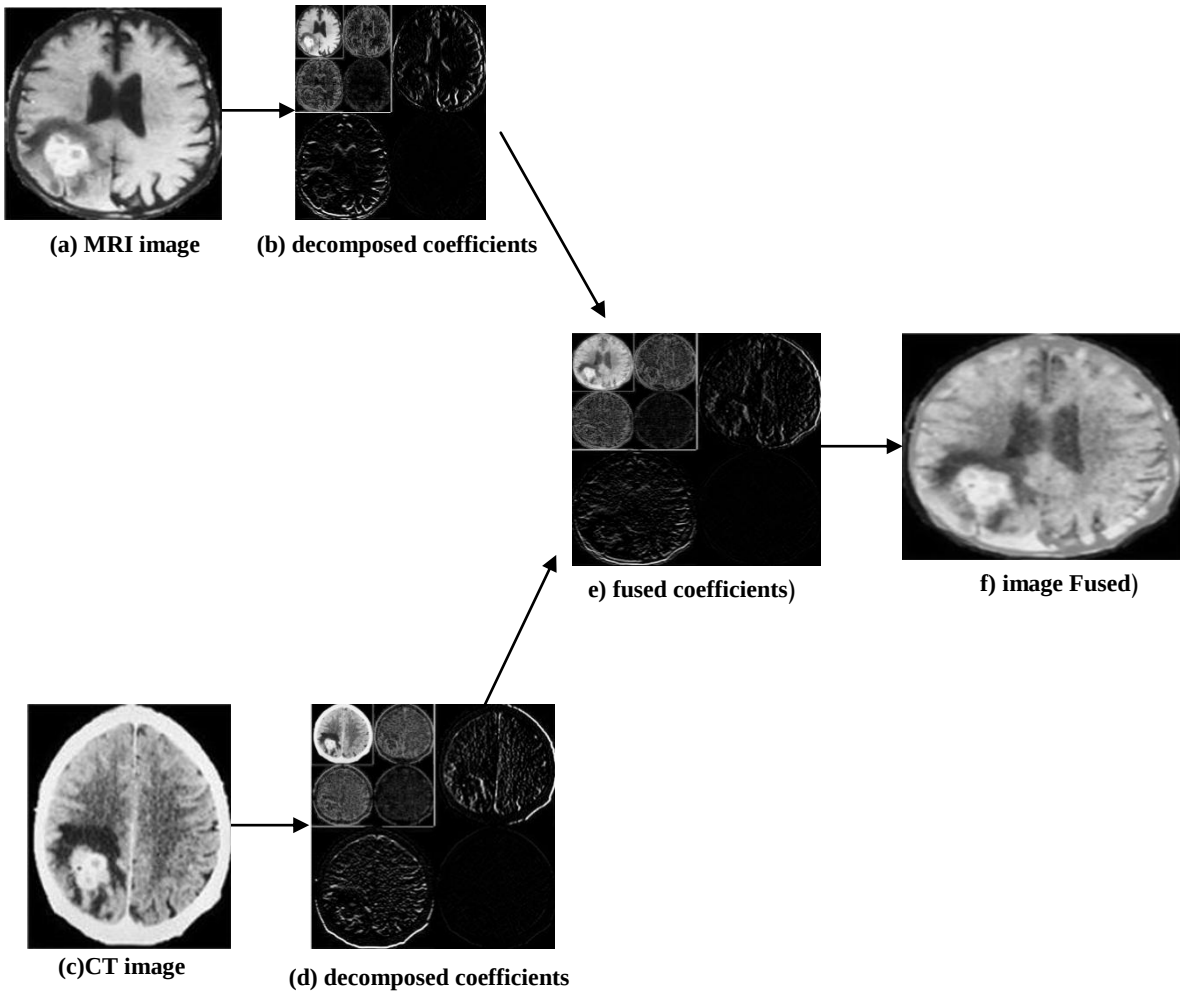

Fig 4.2Block diagram depicting basic image fusion using multire analysis.

Figure (a),(b) shows the decomposition of each image using two separate levels Wave shift.

On each level two are obtained Combinations of coefficients, rounding Low-Low (LL) and details High-Low (HL), Low-High (LH) and High-High (HH). Steps to merge the image using DWT Figure (c),(d) shows the implementation of the conversion of separate wavelets on both input image to create less wavelets division. Figure (e) illustrates smelting each level of decomposition using Different decomposition base .Figure (f) shows the inverse load of the discrete wavelet transform at the level of decomposed fused, which means rebuild the image while

rebuilding the image the fused image. The high accuracy is attained as the method electively extracts the complementary and redundant information from the MR image and CT scan image thereby producing a highly reliable fused output image for detection of tumor .

4.4 Result and analysis

This chapter contains the most important results obtained in this study. The CT and MRI images are combined using the first and second levels of wavelet transform, and the combined image is obtained from CT and MRI scans. The images will improve the accuracy of tumor detection. The quality of the fusion image was measured by calculating PSNR and entropy.

4.4.1 Focus multiple images using the first level wavelet transform

4.4.1.1 first decomposition level for image1:

The algorithm has been applied to MR image as shown in shape (a) and CT image as shown in shape (b) respectively. Shape (c) shows the resultant fusion image using the maximum fusion rule, the figure (4.3) shows the input image and fusion result.

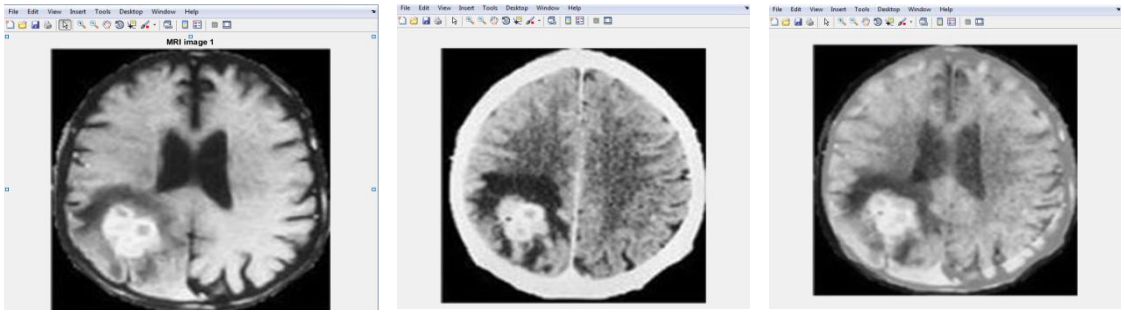

(a)MRI image (Brain) **(b)CT image (Brain)** **(c) Resultant Fused image using maximum fusion rule**

Fig(4.3) Input Images and Fusion Result

Figure(4.4) shows the segmentation results to detect the tumor from the fused image , which is clearly displayed in figure (4.4)(b)then in a figure (4.4)(c) the tumor boundaries are exactly noticed in the brain image due to differences in color from the rest of brain tissues.

(a)Im(age fusion) **(b)Detected fused image** **(c) Tumor**

Fig(4.4) Segmentation results for brain tumor detection

Table (4.1) shows the results of image merging using one level wavelets, and the wavelets are measured based on the signal-to-noise ratio and entropy in tumor detection.

Tab4.1. Performance evaluation of the fused image 'image1' in first level

WAVELETS	bior2.2	coif2	db2	dmey	rbio2.2	sym4	Haar
PSNR	11.1692	11.2073	11.2071	11.1939	11.1652	11.204	11.2456
Entropy	7.4769	7.4562	7.4455	7.4844	7.4338	7.4602	7.4619

Figure (4.5) shows the PSNR values of the results obtained from the different wavelets bior2.2, coif2, db2, dmey, rbio2.2, sym4 and haar respectively, and the higher the PSNR value the better the performance. higher value the PSNR = 11.2456 when Haar waves applied, while less value PSNR = 11.1652 when s applied rbio2.2 waves .

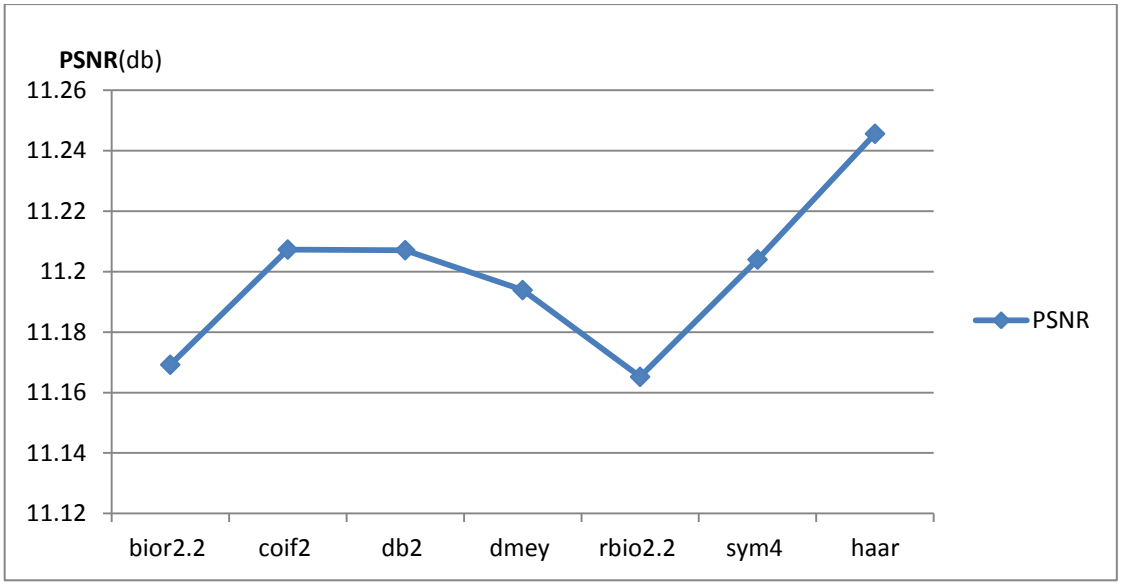

Fig(4.5) Variation of PSNR for different wavelets at first decomposition level

Figure (4.6) shows the Entropy values for the results obtained from different wavelets which are bior2.2, coif2, db2, dmey , rbio2.2, sym4 , haar respectively, and the higher the Entropy value the better the performance. higher value the Entropy= 7.4844 when applied dmey wavelets .

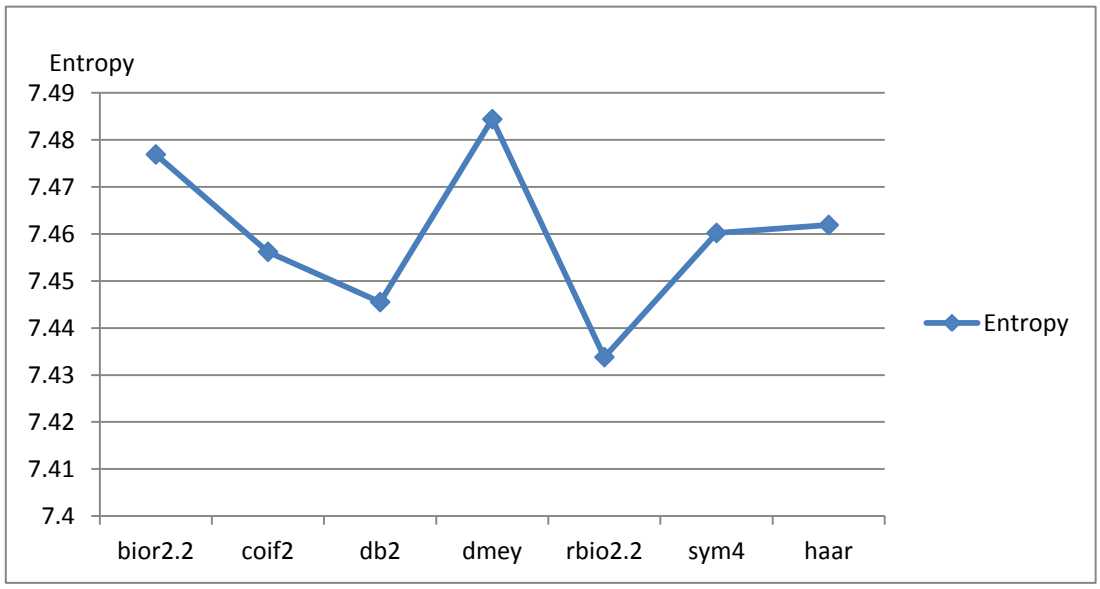

Fig(4.6) Variation of Entropy for different wavelets at first decomposition level

4.4.1.2 first decomposition level for image2:

The algorithm has been applied to MR image as shown in shape (a) and CT image as shown in shape (b) respectively. Shape (c) shows the resultant fusion image using the maximum fusion rule, figure (4.7) shows the input image and fusion result.

(a)MRI image (Brain) **(b)CT image (Brain)** **(c) Resultant Fused image using maximum fusion rule**

Fig(4.7)Input Images and Fusion Result

Figure(4.8) shows the segmentation results to detect the tumor from the fused image , which is clearly displayed in figure (4.8)(b)then in a figure (4.8)(c) the tumor boundaries are exactly noticed in the brain image due to differences in color from the rest of brain tissues.

Image fusion **(b) detected in fused image** **(c) Tumor**

Fig(4.8) Segmentation results for brain tumor detection

In the table (4.2) shows the results of image merging using one level wavelets, and the wavelets are measured based on the signal-to-noise ratio and entropy in tumor detection .

Table (4. 2) Performance evaluation of the fused image 'image2' in first level

WAVELETS	bior2.2	coif2	db2	dmey	rbio2.2	sym4	haar
PSNR	10.0121	10.0384	10.0516	10.034	10.0044	10.0374	10.0678
Entropy	7.1401	7.1366	7.2642	7.3221	7.1609	7.2131	7.2106

Figure (4.9) shows the PSNR values of the results obtained from the different wavelets bior2.2, coif2, db2, dmey, rbio2.2, sym4 and haar respectively, and the higher the PSNR value the better the performance. higher value the PSNR = 10.0678 when Haar waves applied, while less value PSNR = 10.0044 when s applied rbio2.2 waves .

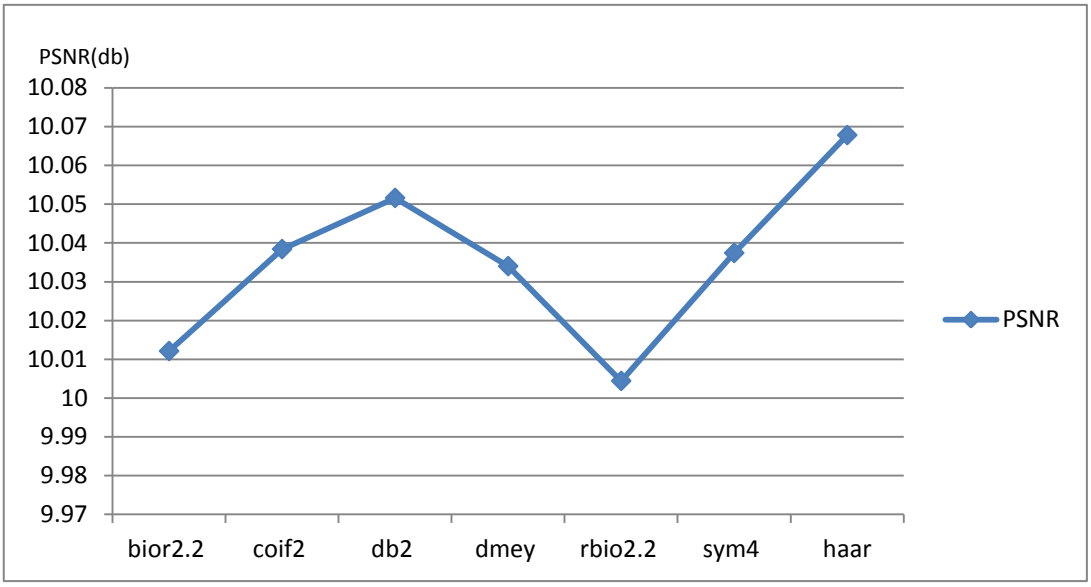

Fig (4.9) Variation of PSNR for different wavelets at first decomposition level

Figure (4.10) shows the Entropy values for the results obtained from different wavelets which are bior2.2, coif2, db2, dmey , rbio2.2, sym4 , haar respectively, and the higher the Entropy value the better the performance. higher value the Entropy= 7.3221 when applied dmey wavelets .

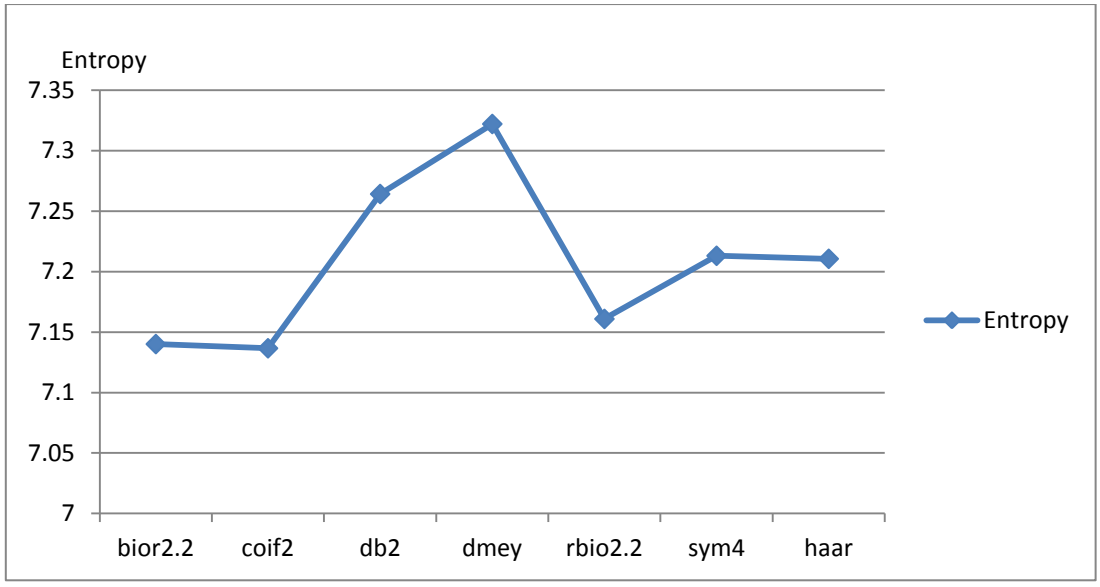

Fig (4.10) Variation of Entropy for different wavelets at first decomposition level

4.4.1.3 first decomposition level for image3:

The algorithm has been applied to MR image as shown in shape (a) and CT image as shown in shape (b) respectively. Shape (c) shows the resultant fusion image using the maximum fusion, the figure (4.11) shows the input image and fusion result.

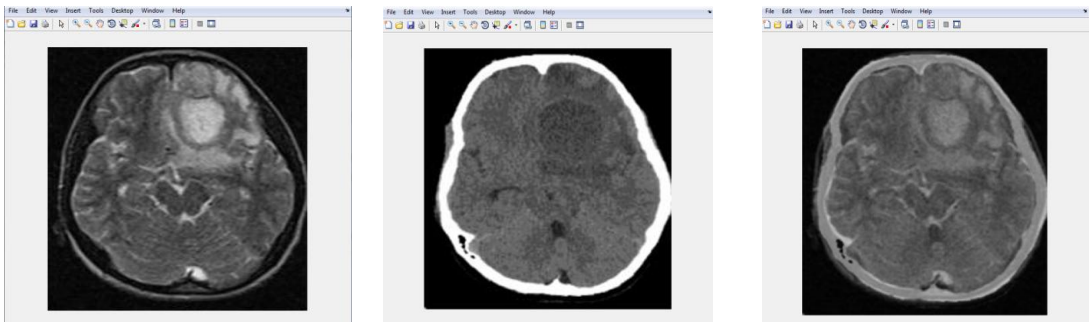

(a)MRI image (Brain) **(b)CT image (Brain)** **(c) Resultant Fused image using maximum fusion rule**

Fig(4.11)Input Images and Fusion Result

Figure(4.12) shows the segmentation results to detect the tumor from the fused image , which is clearly displayed in figure (4.12)(b)then in a figure (4.12)(c) the tumor boundaries are exactly noticed in the brain image due to differences in color from the rest of brain tissues.

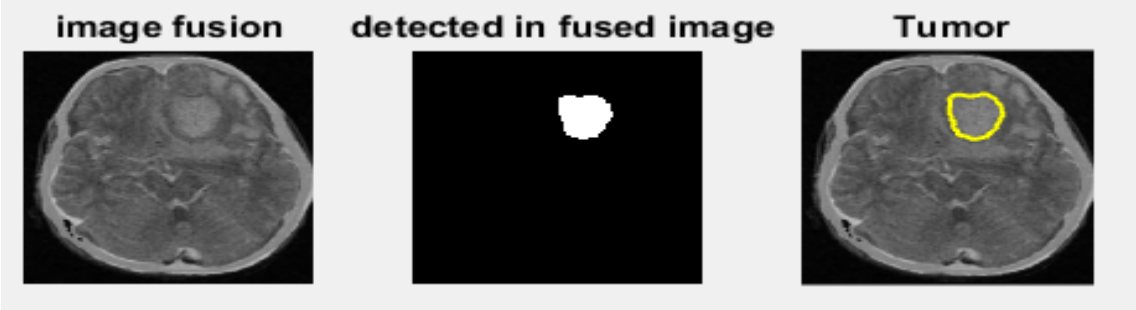

(a) Image fusion **(b) Detected fused image** **(c)Tumor**

Fig(4.12) Segmentation results for brain tumor detection

Table (4.3) shows the results of image merging using one level wavelets, and the wavelets are measured based on the signal-to-noise ratio and entropy in tumor detection

Table (4.3) Performance evaluation of the fused image 'image3' in first level

WAVELETS	bior2.2	coif2	db2	dmey	rbio2.2	sym4	haar
PSNR	10.6179	10.6571	10.6837	10.6527	10.6132	10.6455	10.7219
Entropy	6.8646	6.8894	6.9745	6.9835	6.9369	6.9111	6.9317

Figure (4.13) shows the PSNR values of the results obtained from the different wavelets bior2.2, coif2, db2, dmey, rbio2.2, sym4 and haar respectively, and the higher the PSNR value the better the performance. higher value the PSNR = 10.7219 when Haar waves applied, while less value PSNR = 10.6132 when s applied rbio2.2 waves .

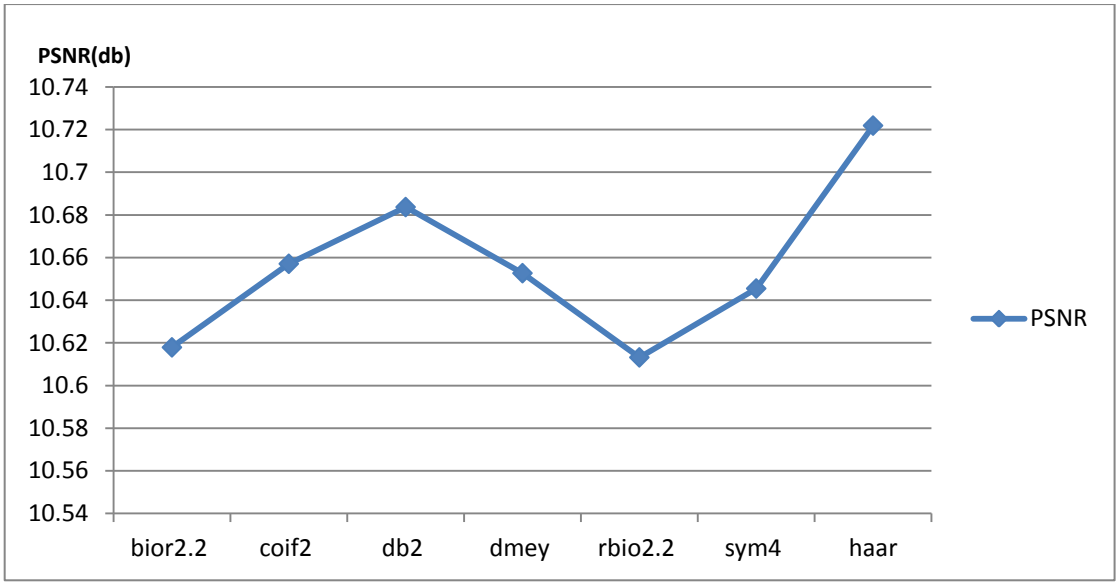

Fig(4.13) Variation of PSNR for different wavelets at first decomposition level

Figure (4.14) shows the Entropy values for the results obtained from different wavelets which are bior2.2, coif2, db2, dmey , rbio2.2, sym4 , haar respectively, and the higher the Entropy value the better the performance. higher value the Entropy= 6.9835 when applied dmey wavelets .

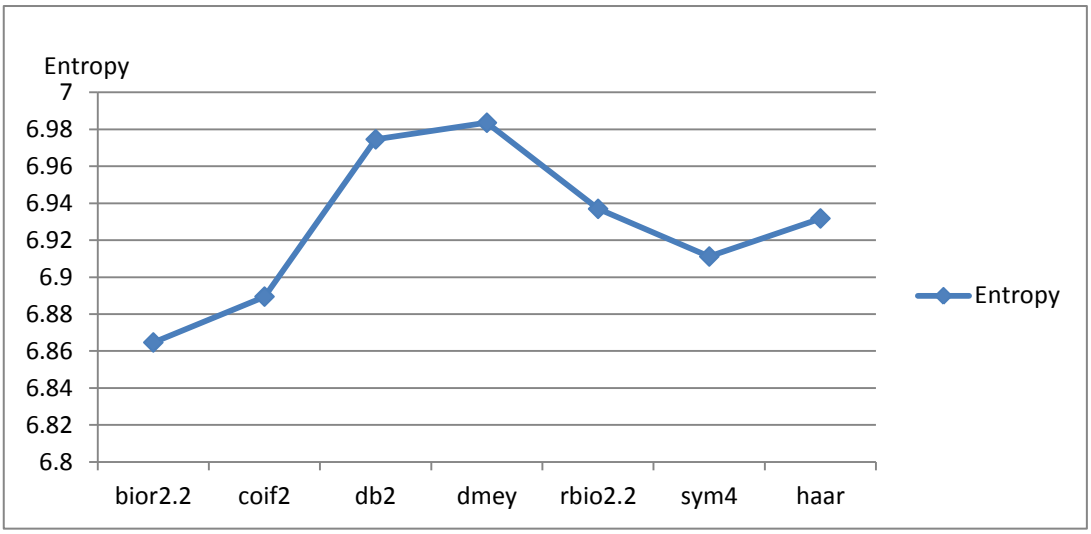

Fig(4.14) Variation of Entropy for different wavelets at first decomposition level

4.4.1.4 first decomposition level for image4:

The algorithm has been applied to MR image as shown in shape (a) and CT image as shown in shape (b) respectively. Shape (c) shows the

resultant fusion image using the maximum fusion, the figure (4.15) shows the input image and fusion result.

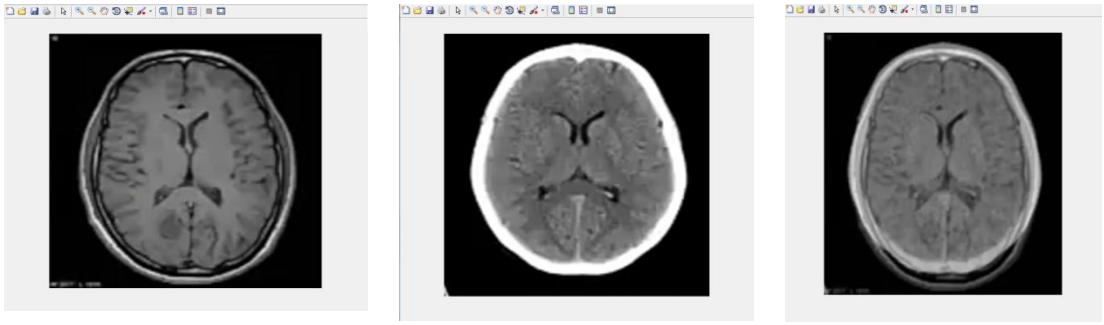

(a)MRI image (Brain) **(b)CT image (Brain)** **(c) Resultant Fused image using maximum fusion rule**

Fig(4.15) Input Images and Fusion Result

Figure (4.16) shows the segmentation results to detect the tumor from the combined image, and the image can be considered tumor-free if all pixels in the resulting image have zero values in this case there is no ubnormal behavior in the tissues as in Figure(4.16)(b) ,so this condition is considered tumor free as shown in Fig (4.16)(c).

(a)Image fusion **(b)detected fused image** **(c)Tumor**

Fig(4.16) Segmentation results for brain tumor detection

In the table (4.4) shows the results of image merging using one level wavelets, and the wavelets are measured based on the signal-to-noise ratio and entropy in tumor detection.

Table (4.4) Performance evaluation of the fused image 'image4' in first level

WAVELETS	bior2.2	coif2	db2	dmey	rbio2.2	sym4	haar
PSNR	12.1367	12.1417	12.1549	12.1280	12.0799	12.1291	12.1795
Entropy	6.0264	5.9778	6.0287	6.1929	5.9603	6.0317	5.9479

Figure (4.17) shows the PSNR values of the results obtained from the different wavelets bior2.2, coif2, db2, dmey, rbio2.2, sym4 and haar respectively, and the higher the PSNR value the better the performance. higher value the PSNR = 12.1795when Haar waves applied, while less value PSNR = 12.0799when s applied rbio2.2 waves .

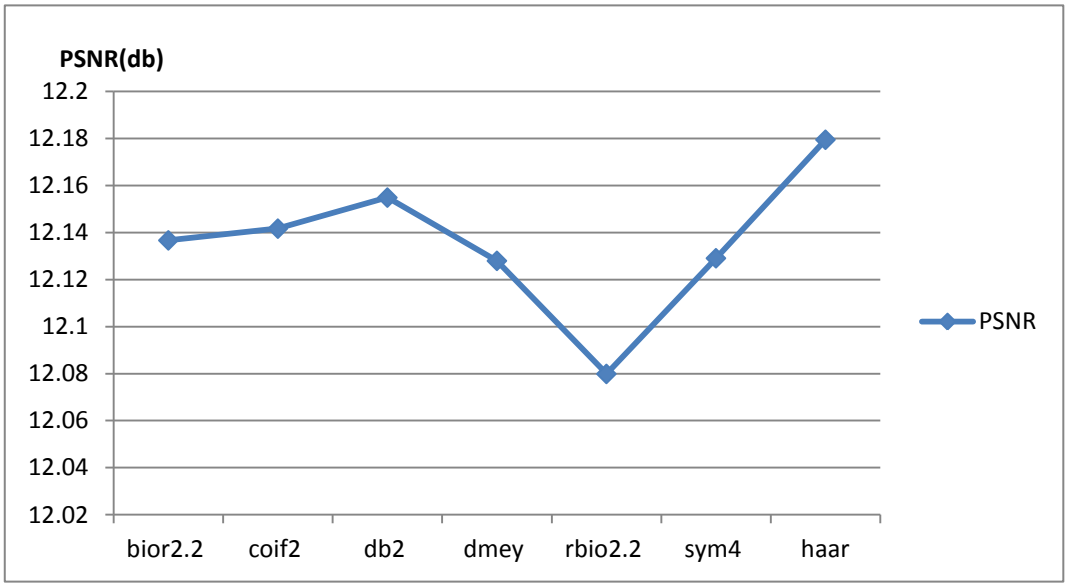

Fig (4.17) Variation of PSNR for different wavelets at first decomposition level

Figure (4.18) shows the Entropy values for the results obtained from different wavelets which are bior2.2, coif2, db2, dmey , rbio2.2, sym4 , haar respectively, and the higher the Entropy value the better the performance. higher value the Entropy= 6.1929 when applied dmey wavelets .

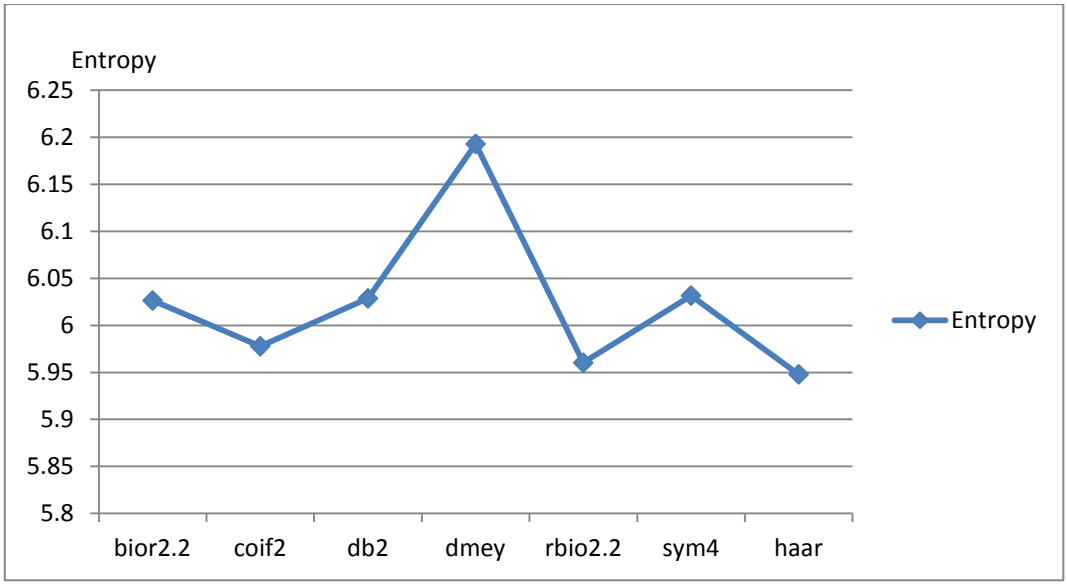

Fig(4.18) Variation of Entropy for different wavelets at first decomposition level

4.4.1.5 first decomposition level for image5:

The algorithm has been applied to MR image as shown in shape (a) and CT image as shown in shape (b) respectively. Shape (c) shows the resultant fusion image using the maximum fusion, the figure (4.19) shows the input image and fusion result.

(a)MRI image (Brain) **(b)CT image (Brain)** **(c) Resultant Fused image using maximum fusion rule**

Fig(4.19) Input Images and Fusion Result

Figure (4.20) shows the segmentation results to detect the tumor from the combined image, and the image can be considered tumor-free if all pixels in the resulting image have zero values in this case there is no ubnormal behavior in the tissues as in Figure(4.20)(b) ,so this condition is considered tumor free as shown in Fig (4.20)(c).

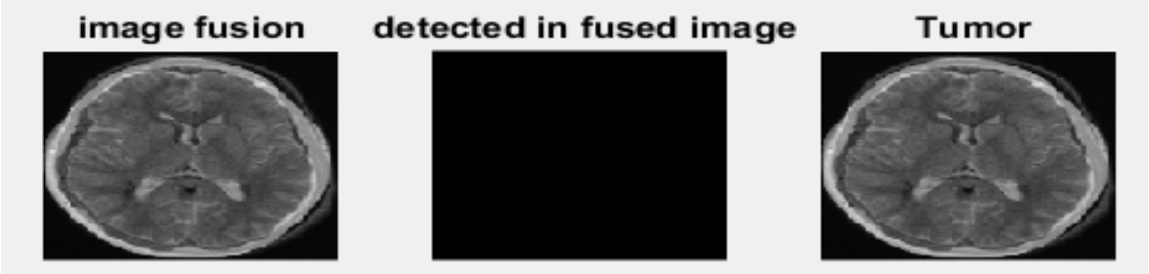

(a)Image fusion **(b)detected fused image** **(c)Tumor**

Fig(4.20) Segmentation results for brain tumor detection

In the table (4.5) shows the results of image merging using one level wavelets, and the wavelets are measured based on the signal-to-noise ratio and entropy in tumor detection.

Table (4.5) Performance evaluation of the fused image 'image5' in first level

WAVELETS	bior2.2	coif2	db2	dmey	rbio2.2	sym4	haar
PSNR	11.7913	11.8323	11.8336	11.8294	11.7759	11. 940	11.8679
Entropy	6.8860	6.8910	6.9767	7.0078	6.9170	6.9260	6.9351

Figure (4.21) shows the PSNR values of the results obtained from the different wavelets bior2.2, coif2, db2, dmey, rbio2.2, sym4 and haar respectively, and the higher the PSNR value the better the performance. higher value the PSNR = 11.8679 when Haar waves applied, while less value PSNR = 11.7759 when s applied rbio2.2 waves .

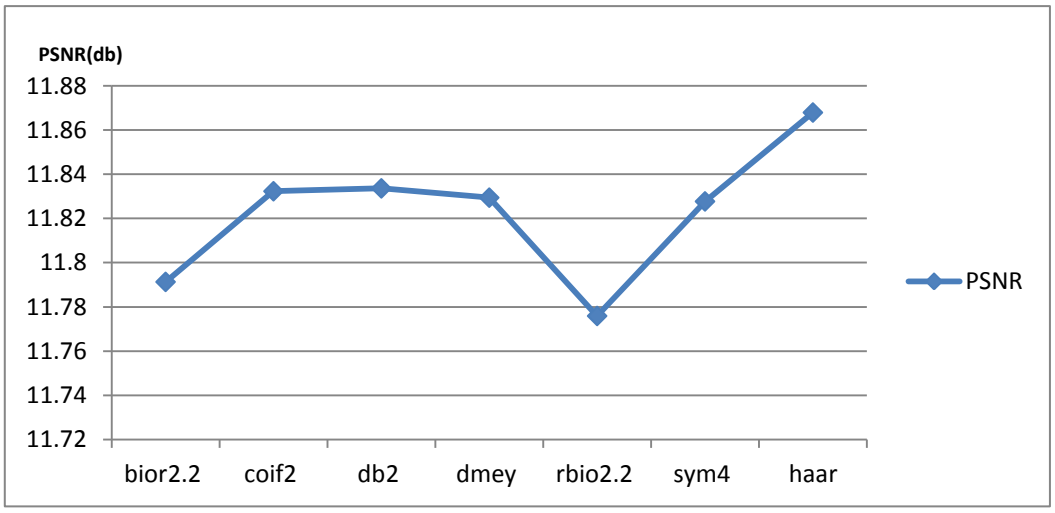

Fig (4.21) Variation of PSNR for different wavelets at first decomposition level

Figure (4.22) shows the Entropy values for the results obtained from different wavelets which are bior2.2, coif2, db2, dmey , rbio2.2, sym4 , haar respectively, and the higher the Entropy value the better the performance. higher value the Entropy= 7.0078 when applied dmey wavelets .

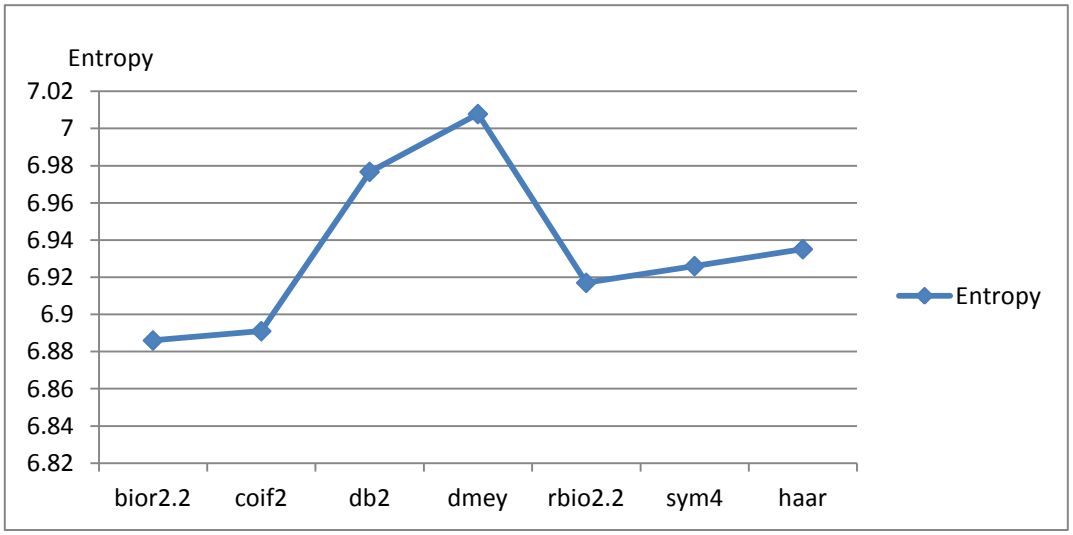

Fig(4.22) Variation of Entropy for different wavelets at first decomposition level

4.4.2 Focus multiple images using the second level wavelet transform

4.4.2.1 Second decomposition level for image1:

The algorithm has been applied to MR image as shown in shape (a) and CT image as shown in shape (b) respectively. Shape (c) shows the resultant fusion image using the maximum fusion, the figure (4.23) shows the input image and fusion result.

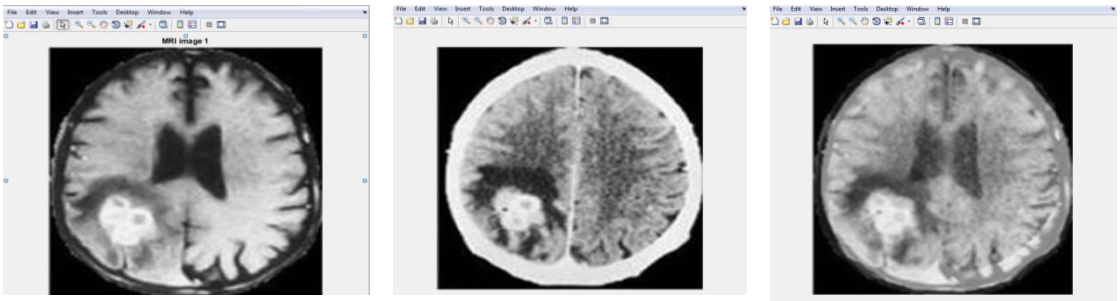

(a)MRI image (Brain) **(b)CT image (Brain)** **(c) Resultant Fused image using maximum fusion rule**

Fig(4.23) Input Images and Fusion Result

Figure(4.23) shows the segmentation results to detect the tumor from the fused image , which is clearly displayed in figure (4.23)(b)then in a figure (4.23)(c) the tumor boundaries are exactly noticed in the brain image due to differences in color from the rest of brain tissues.

Image fusion **(b) detected fused image** **(c) Tumor**

Fig(4.24) Segmentation results for brain tumor detection

In the table (4.6) shows the results of image merging using two level wavelets, and the wavelets are measured based on the signal-to-noise ratio and entropy in tumor detection.

Table (4.6) Performance evaluation of the fused image 'image1'in second level

WAVELETS	bior2.2	coif2	db2	dmey	rbio2.2	sym4	haar
PSNR	11.1891	11.3254	11.3378	11.2821	10.9375	11.3045	11.4073
Entropy	7.5382	7.5117	7.4709	7.5640	7.4301	7.5101	7.425

Figure (4.25) shows the PSNR values of the results obtained from the different wavelets bior2.2, coif2, db2, dmey, rbio2.2, sym4 and haar respectively, and the higher the PSNR value the better the performance. higher value the PSNR = 11.4073when Haar waves applied, while less value PSNR = 10.9375 when s applied rbio2.2 waves .

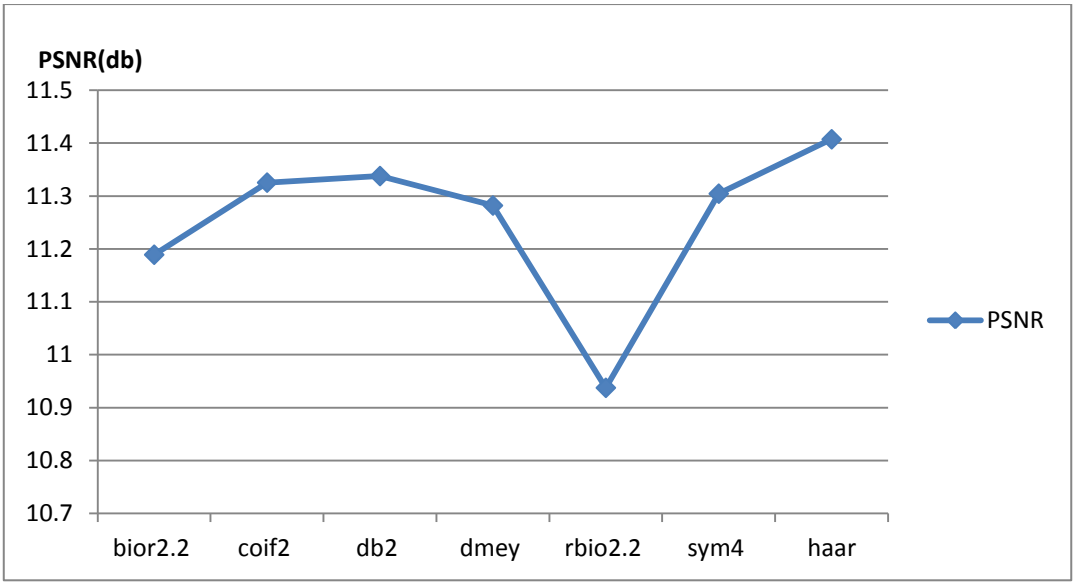

Fig (4.25) Variation of PSNR for different wavelets at second decomposition level

Figure (4.26) shows the Entropy values for the results obtained from different wavelets which are bior2.2, coif2, db2, dmey , rbio2.2, sym4 , haar respectively, and the higher the Entropy value the better the performance. higher value the Entropy= 7.5640 when applied dmey wavelets .

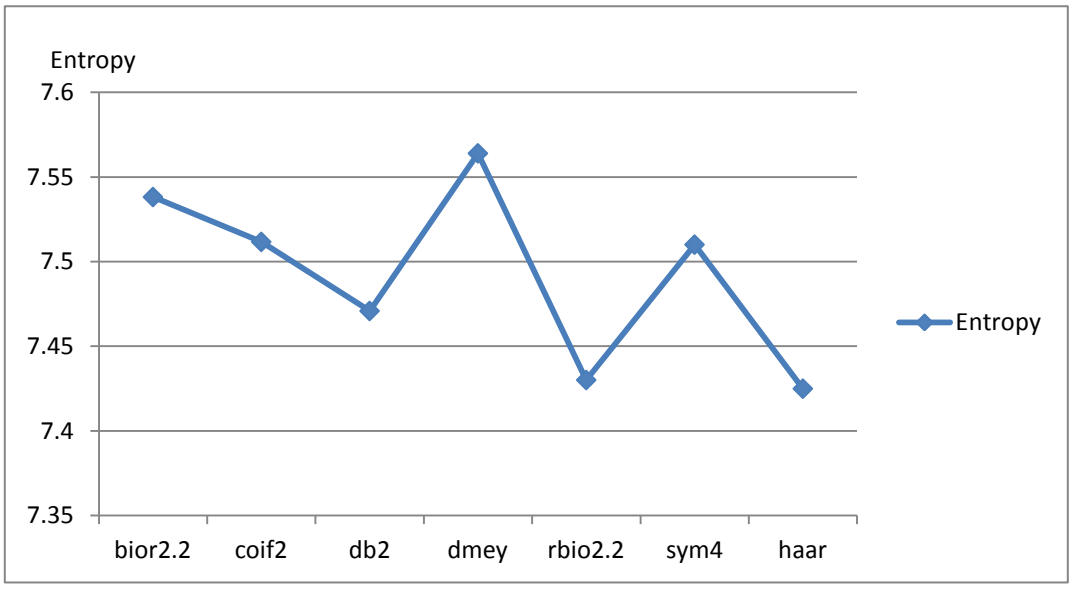

Fig (4.26) Variation of Entropy for different wavelets at second decomposition level

4.4.2.2 Second decomposition level for image2:

The algorithm has been applied to MR image as shown in shape (a) and CT image as shown in shape (b) respectively. Shape (c) shows the resultant fusion image using the maximum fusion, the figure (4.27) shows the input image and fusion result.

(a)MRI image (Brain) **(b)CT image (Brain)** **(c) Resultant Fused image using maximum fusion rule**

Fig(4.27) Input Images and Fusion Result

Figure(4.28) shows the segmentation results to detect the tumor from the fused image , which is clearly displayed in figure (4.28)(b)then in a figure (4.28)(c) the tumor boundaries are exactly noticed in the brain image due to differences in color from the rest of brain tissues.

(a)Image fusion **(b)detected in fused image** **(c)Tumor**

Fig(4.28) Segmentation results for brain tumor detection

In the table (4.7) shows the results of image merging using two level wavelets, and the wavelets are measured based on the signal-to-noise ratio and entropy in tumor detection.

Table (4.7) Performance evaluation of the fused image 'image2' in second level

WAVELETS	bior2.2	coif2	db2	dmey	rbio2.2	sym4	haar
PSNR	10.0578	10.1391	10.1663	10.1324	9.8036	10.1183	10.194
Entropy	7.3674	7.3205	7.4722	7.5244	7.3581	7.4068	7.3011

Figure (4.29) shows the PSNR values of the results obtained from the different wavelets bior2.2, coif2, db2, dmey, rbio2.2, sym4 and haar respectively, and the higher the PSNR value the better the performance. higher value the PSNR = 10.194 when Haar waves applied, while less value PSNR = 9.8036 when s applied rbio2.2 waves .

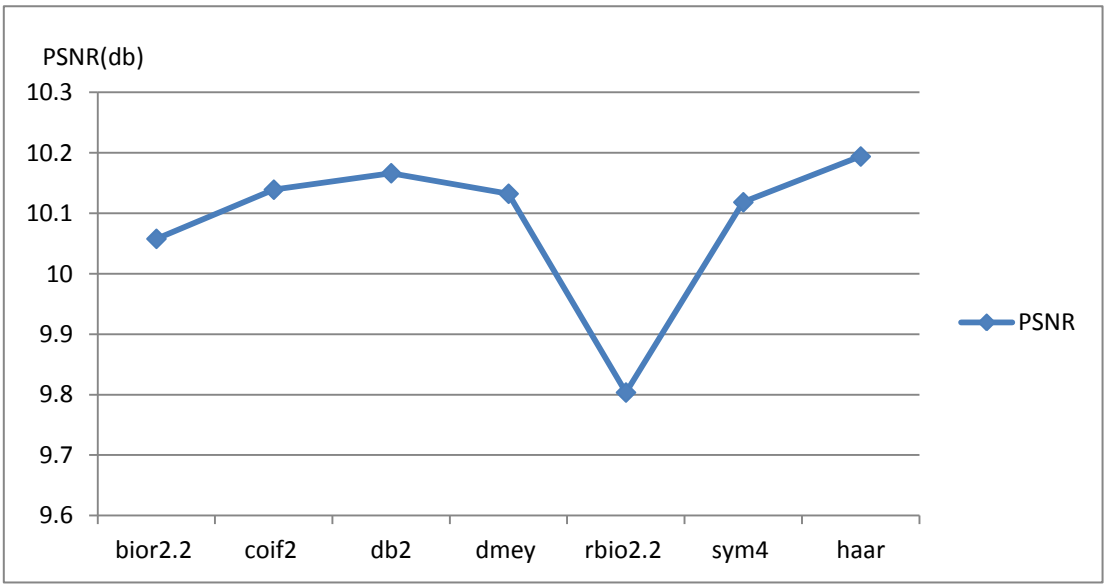

Fig (4.29) Variation of PSNR for different wavelets at second decomposition level

Figure (4.30) shows the Entropy values for the results obtained from different wavelets which are bior2.2, coif2, db2, dmey , rbio2.2, sym4 , haar respectively, and the higher the Entropy value the better the performance. higher value the Entropy= 7.5244 when applied dmey wavelets .

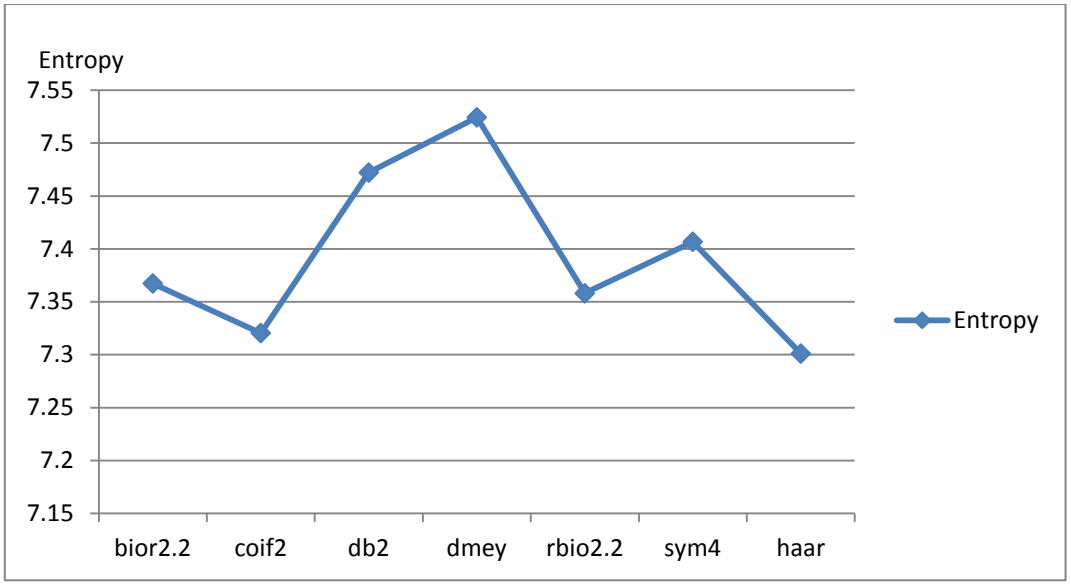

Fig(4.30) Variation of Entropy for different wavelets at second decomposition level

4.4.2.3 Second decomposition level for image3:

The algorithm has been applied to MR image as shown in shape (a) and CT image as shown in shape (b) respectively. Shape (c) shows the resultant fusion image using the maximum fusion, the figure (4.31) shows the input image and fusion result.

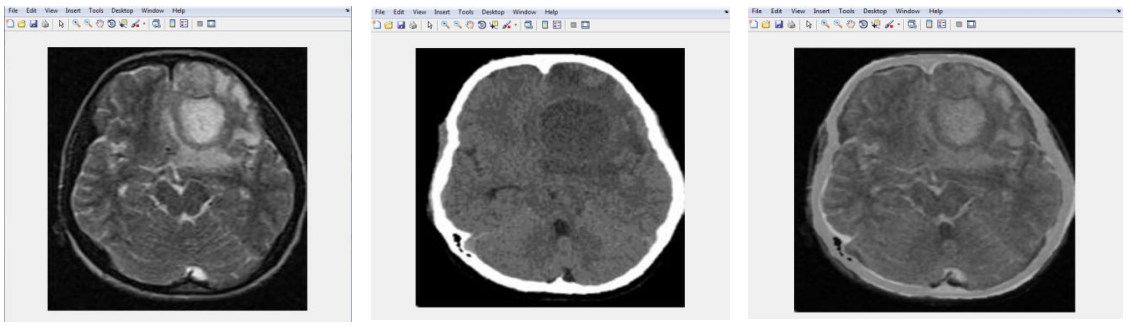

(a)MRI image (Brain) **(b)CT image (Brain)** **(c) Resultant Fused image using maximum fusion rule**

Fig(4.31) Input Images and Fusion Result

Figure(4.32) shows the segmentation results to detect the tumor from the fused image , which is clearly displayed in figure (4.32)(b)then in a figure (4.32)(c) the tumor boundaries are exactly noticed in the brain image due to differences in color from the rest of brain tissues.

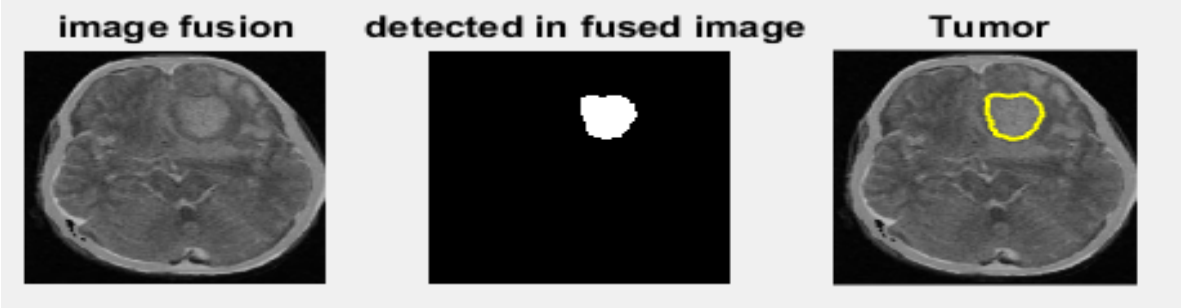

(a)Image fusion **(b)detected in fused image** **(c) Tumor**

Fig(4.32) Segmentation results for brain tumor detection

In the table (4.8) shows the results of image merging using two level wavelets, and the wavelets are measured based on the signal-to-noise ratio and entropy in tumor detection

Table(4.8) Performance evaluation of the fused image 'image3' in second level

WAVELETS	bior2.2	coif2	db2	dmey	rbio2.2	sym4	haar
PSNR	10.7542	10.8552	10.8418	10.7936	10.404	10.8053	10.9391
Entropy	7.1316	7.0716	7.1845	7.2687	7.0895	7.1440	7.0798

Figure (4.33) shows the PSNR values of the results obtained from the different wavelets bior2.2, coif2, db2, dmey, rbio2.2, sym4 and haar respectively, and the higher the PSNR value the better the performance. higher value the PSNR = 10.9391when Haar waves applied, while less value PSNR = 10.404 when s applied rbio2.2 waves .

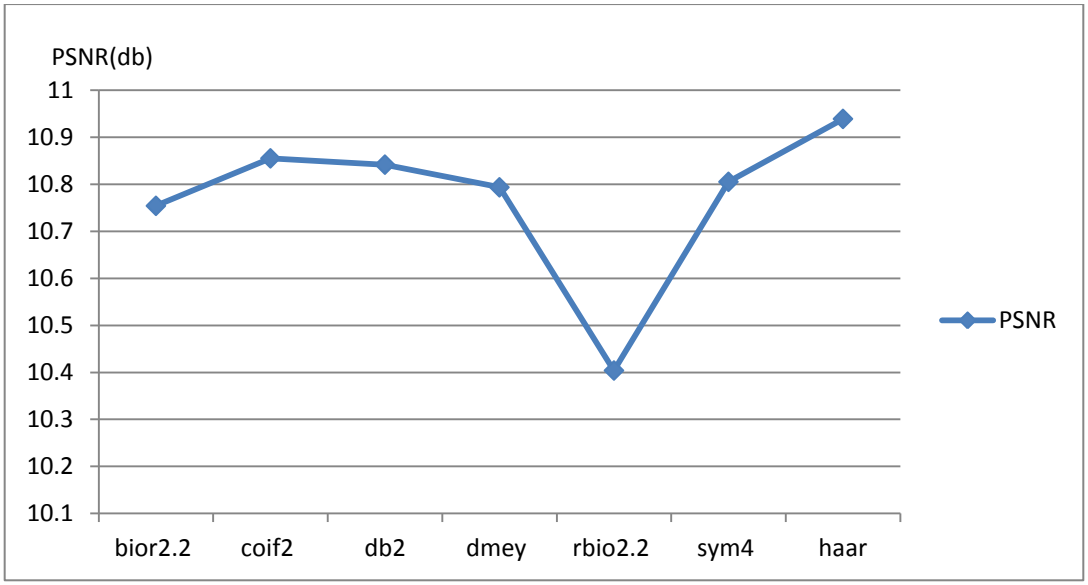

Fig(4.33) Variation of PSNR for different wavelets at second decomposition level

Figure (4.34) shows the Entropy values for the results obtained from different wavelets which are bior2.2, coif2, db2, dmey , rbio2.2, sym4 , haar respectively, and the higher the Entropy value the better the performance. higher value the Entropy= 7.2687 when applied dmey wavelets .

Fig (4.34) Variation of Entropy for different wavelets at second decomposition level

4.4.2.4 Second decomposition level for image4:

The algorithm has been applied to MR image as shown in shape (a) and CT image as shown in shape (b) respectively. Shape (c) shows the resultant fusion image using the maximum fusion, the figure (4.35) shows the input image and fusion result.

(a)MRI image (Brain) (b)CT image (Brain) (c) Resultant Fused image using maximum fusion rule

Fig(4.35) Input Images and Fusion Result

Figure (4.36) shows the segmentation results to detect the tumor from the combined image, and the image can be considered tumor-free if all pixels in the resulting image have zero values in this case there is no ubnormal behavior in the tissues as in Figure(4.36)(b) ,so this condition is considered tumor free as shown in Fig (4.36)(c).

(a)Image fusion **(b)detected in fused image** **(c)Tumor**

Fig(4.36) Segmentation results for brain tumor detection

In the table (4.9) shows the results of image merging using two level wavelets, and the wavelets are measured based on the signal-to-noise ratio and entropy in tumor detection

Table (4.9) Performance evaluation of the fused image 'image4' in second level

WAVELETS	bior2.2	coif2	db2	Dmey	rbio2.2	sym4	haar
PSNR	12.2245	12.2603	12.2608	12.2437	11.2347	12.2055	12.3218
Entropy	6.4515	6.2966	6.3661	6.5648	6.2167	6.3690	6.0978

Figure (4.37) shows the PSNR values of the results obtained from the different wavelets bior2.2, coif2, db2, dmey, rbio2.2, sym4 and haar respectively, and the higher the PSNR value the better the performance. higher value the PSNR = 10.9391when Haar waves applied, while less value PSNR = 10.404 when s applied rbio2.2 waves .

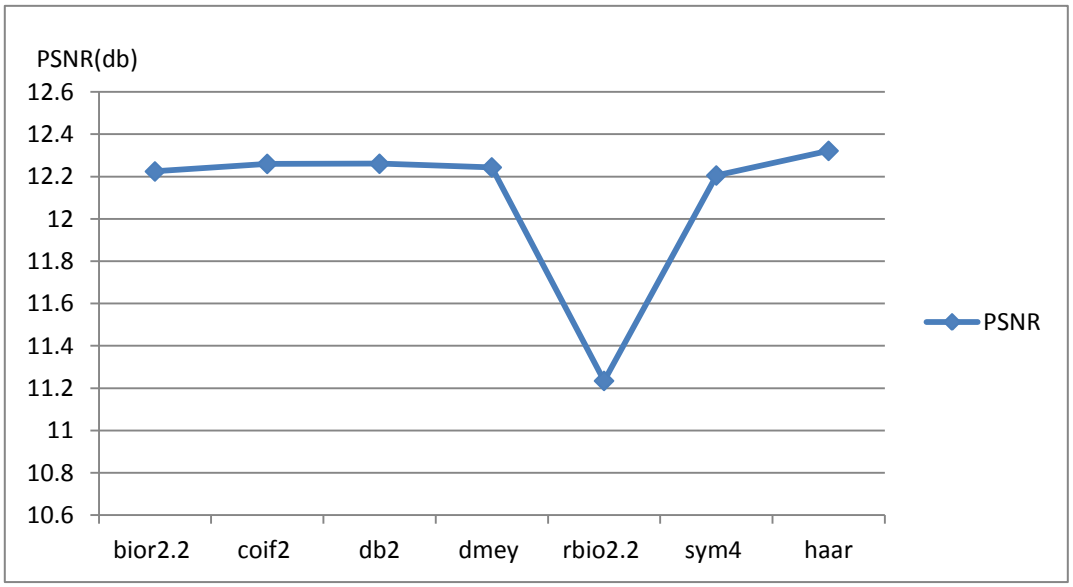

Fig 4.37. Variation of PSNR for different wavelets at second decomposition level

Figure (4.38) shows the Entropy values for the results obtained from different wavelets which are bior2.2, coif2, db2, dmey , rbio2.2, sym4 , haar respectively, and the higher the Entropy value the better the performance. higher value the Entropy= 6.5648 when applied dmey wavelets .

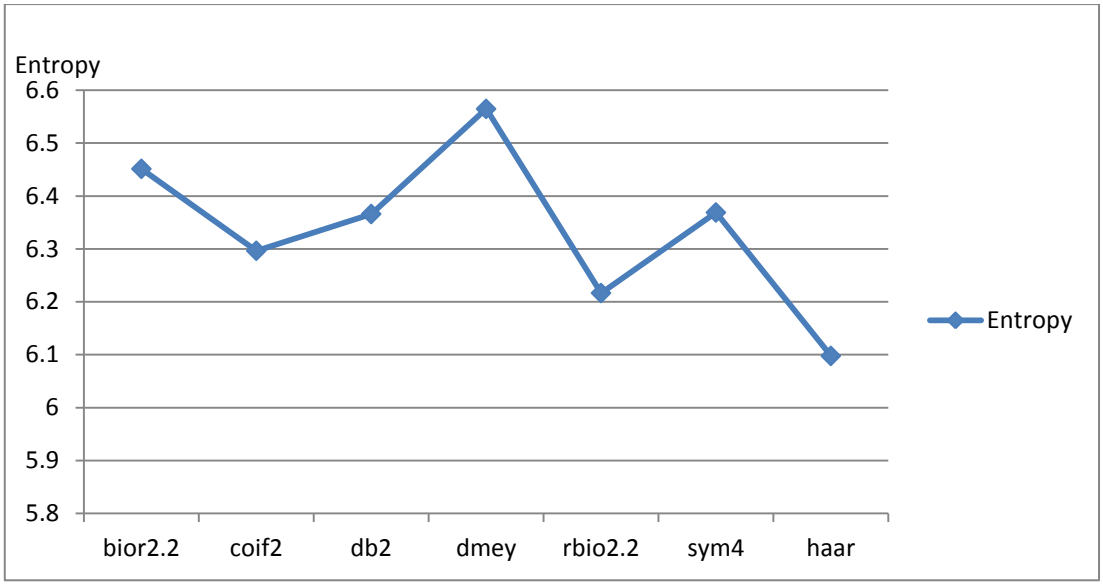

Fig 4.38: Variation of Entropy for different wavelets at second decomposition level

4.4.2.5 Second decomposition level for image5:

The algorithm has been applied to MR image as shown in shape (a) and CT image as shown in shape (b) respectively. Shape (c) shows the resultant fusion image using the maximum fusion, the figure (4.39) shows the input image and fusion result.

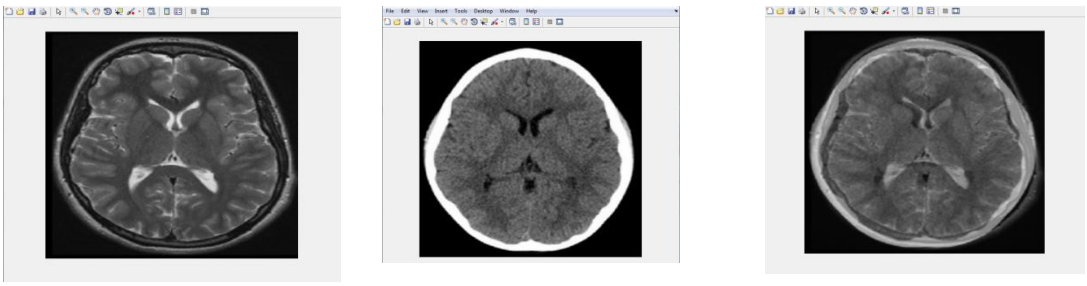

(a)MRI image (Brain) (b)CT image (Brain) (c) Resultant Fused image using maximum fusion rule

Fig(4.39) Input Images and Fusion Result

Figure (4.40) shows the segmentation results to detect the tumor from the combined image, and the image can be considered tumor-free if all pixels in the resulting image have zero values in this case there is no ubnormal behavior in the tissues as in Figure(4.40)(b) ,so this condition is considered tumor free as shown in Fig (4.40)(c).

(a)Image fusion **(b)detected in fused image** **(c)Tumor**

Fig(4.40) Segmentation results for brain tumor detection

In the table (4.10) shows the results of image merging using two level wavelets, and the wavelets are measured based on the signal-to-noise ratio and entropy in tumor detection

Table(4.10) Performance evaluation of the fused image 'image5' in second level.

WAVELETS	bior2.2	coif2	db2	Dmey	rbio2.2	sym4	haar
PSNR	11.8585	11.9786	11.9627	11.9144	11.4897	11.8277	12.0840
Entropy	7.1668	7.1204	7.1679	7.2525	7.1243	7.1316	7.0418

Figure (4.41) shows the PSNR values of the results obtained from the different wavelets bior2.2, coif2, db2, dmey, rbio2.2, sym4 and haar respectively, and the higher the PSNR value the better the performance. higher value the PSNR = 12.0840 when Haar waves applied, while less value PSNR = 11.4897 when s applied rbio2.2 waves .

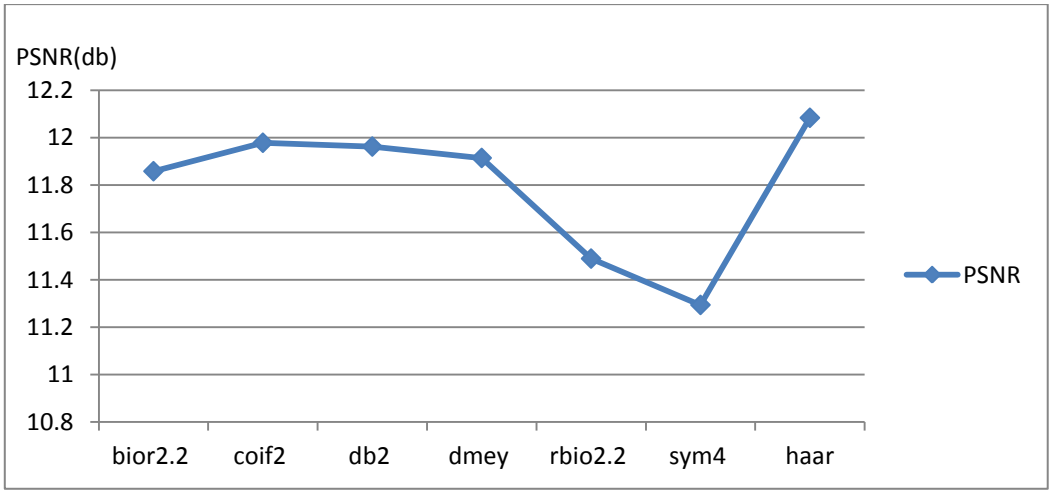

Fig 4.41. Variation of PSNR for different wavelets at second decomposition level

Figure (4.42) shows the Entropy values for the results obtained from different wavelets which are bior2.2, coif2, db2, dmey , rbio2.2, sym4 , haar respectively, and the higher the Entropy value the better the performance. higher value the Entropy= 7.2525 when applied dmey wavelets .

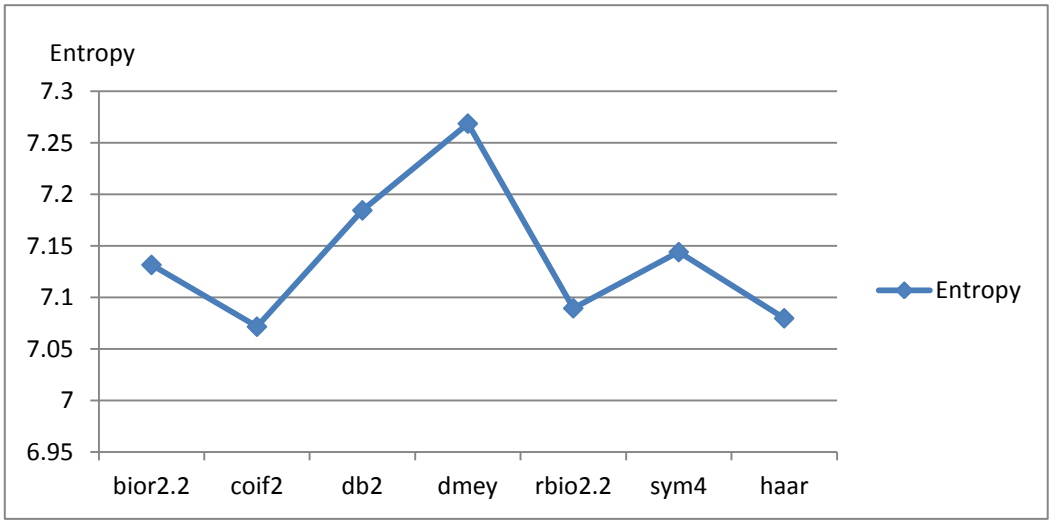

Fig 4.42: Variation of Entropy for different wavelets at second decomposition level

4.5 Comparison of the first and second levels in terms of the difference in the PSNR.

Figure (4.43) shows the PSNR values for the value of results obtained from the 'image 1' in the first and second levels from different waves in bior2.2, coif2, db2, dmey, rbio2.2, sym4 and haar waves. It was clearly noted that the results of the PSNR were better at the second level, with the exception of the wavelet rbio2.2 , where the PSNR value in the first level was equal to 11.1652 and the PSNR value in the second level was equal to 10.9375. This is due to the level of decomposition used to transform the wavelets, Increased depth of analysis leads to better results in most types of wavelets used for detection of tumor .

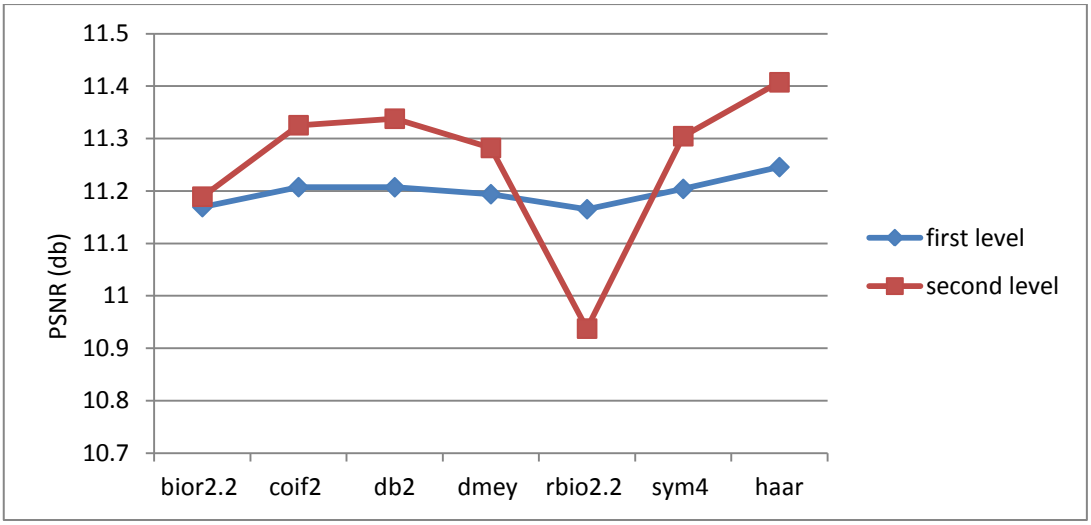

Fig4.43: Variation of PSNR for different wavelets at first and second decomposition level for image1

Figure(4.44) shows the PSNR values for the value of results obtained from the 'image 2' in the first and second levels from different waves in bior2.2, coif2, db2, dmey, rbio2.2, sym4 and haar waves. It was clearly noted that the results of the PSNR were better at the second level, with the exception of the wavelet rbio2.2 , where the PSNR value in the first level was equal to 10.0044 and the PSNR value in the second level was equal to 9.8036. This is due to the level of decomposition used to transform the wavelets, Increased depth of analysis leads to better results in most types of wavelets used for detection of tumor .

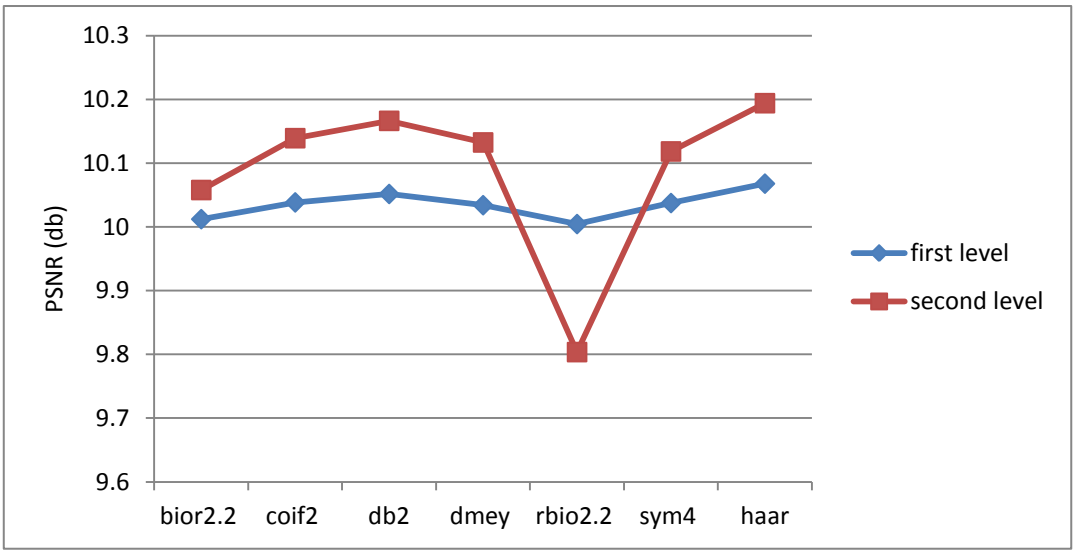

Fig4.44: Variation of PSNR for different wavelets at first and second decomposition level for image2

Figure (4.45) shows the PSNR values for the value of results obtained from the 'image 3'in the first and second levels from different waves in bior2.2, coif2, db2, dmey, rbio2.2, sym4 and haar waves. It was clearly noted that the results of the PSNR were better at the second level, with the exception of the wavelet rbio2.2 , where the PSNR value in the first level was equal to 10.6132 and the PSNR value in the second level was equal to 10.404. This is due to the level of decomposition used to transform the wavelets, Increased depth of analysis leads to better results in most types of wavelets used for detection of tumor .

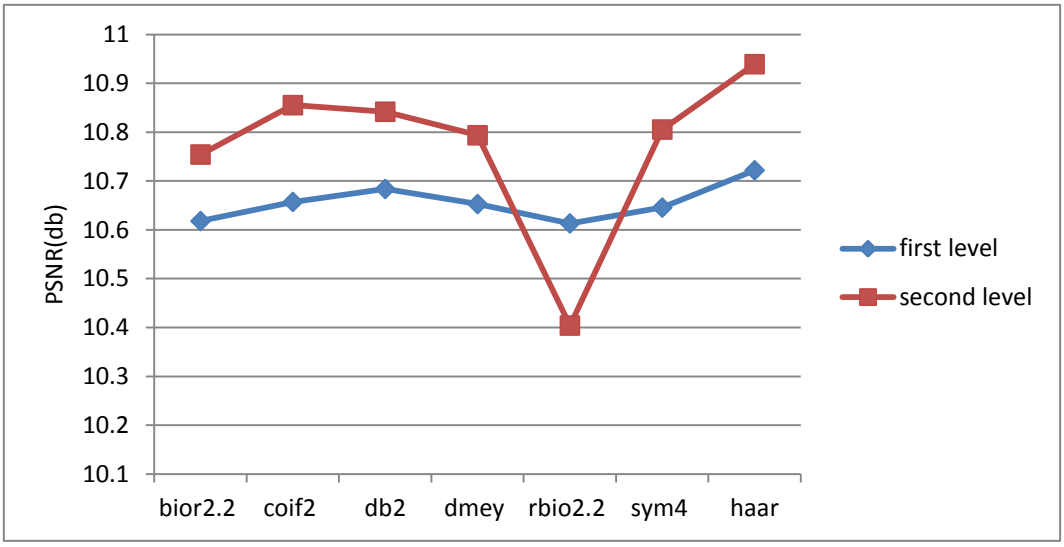

Fig4.45: Variation of PSNR for different wavelets at first and second decomposition level for image3

Figure (4.46) shows the PSNR values for the value of results obtained from the 'image 4' in the first and second levels from different waves in bior2.2, coif2, db2, dmey, rbio2.2, sym4 and haar waves. It was clearly noted that the results of the PSNR were better at the second level, with the exception of the wavelet rbio2.2 , where the PSNR value in the first level was equal to 12.0799 and the PSNR value in the second level was equal to 11.2347. This is due to the level of decomposition used to

transform the wavelets, Increased depth of analysis leads to better results in most types of wavelets used for detection of tumor .

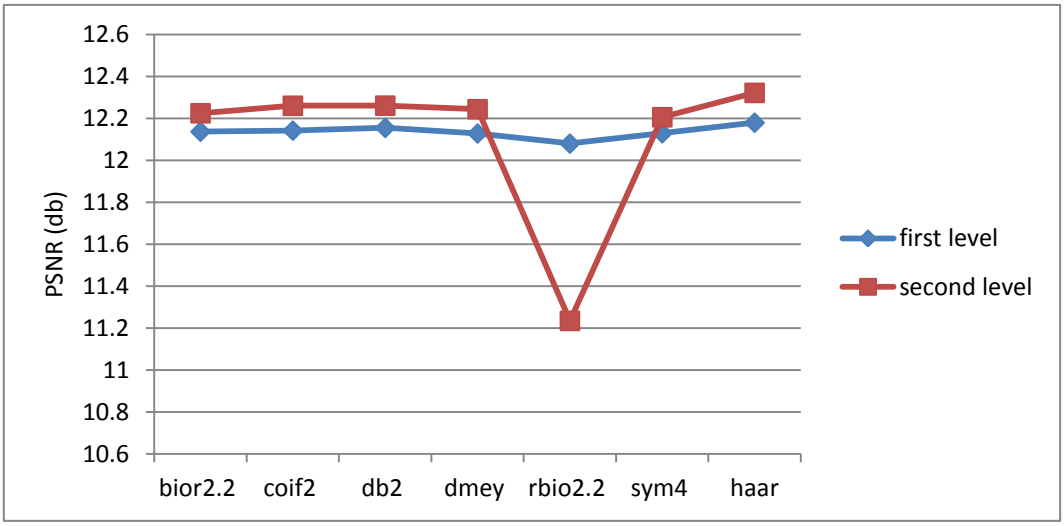

Fig4.46: Variation of PSNR for different wavelets at first and second decomposition level for image4

Figure(4.47) shows the PSNR values for the value of results obtained from the 'image 5' in the first and second levels from different waves in bior2.2, coif2, db2, dmey, rbio2.2, sym4 and haar waves. It was clearly noted that the results of the PSNR were better at the second level, with the exception of the wavelet rbio2.2 and sym4 , where the PSNR value in the first level was equal to 11.7759 and the PSNR value in the second level was equal to 11.4897. This is due to the level of decomposition used to transform the wavelets, Increased depth of analysis leads to better results in most types of wavelets used for detection of tumor .

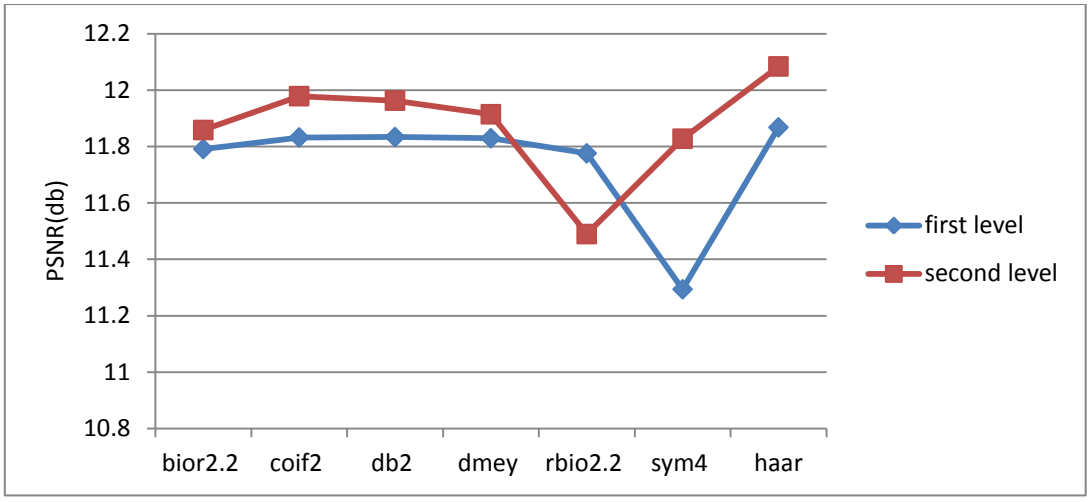

Fig4.47: Variation of PSNR for different wavelets at first and second decomposition level for image5

4.6 Comparison of the first and second levels in terms of the difference in the Entropy.

Figure(4.48) shows the Entropy values for the value of results obtained from the first case in the first and second levels from different waves in bior2.2, coif2, db2, dmey, rbio2.2, sym4 and haar. It was clearly noted that Entropy results were better at the second level . This is due to the level of decomposition used to transform the wavelets, Increased depth of analysis leads to better results in most types of wavelets used for detection of tumor .

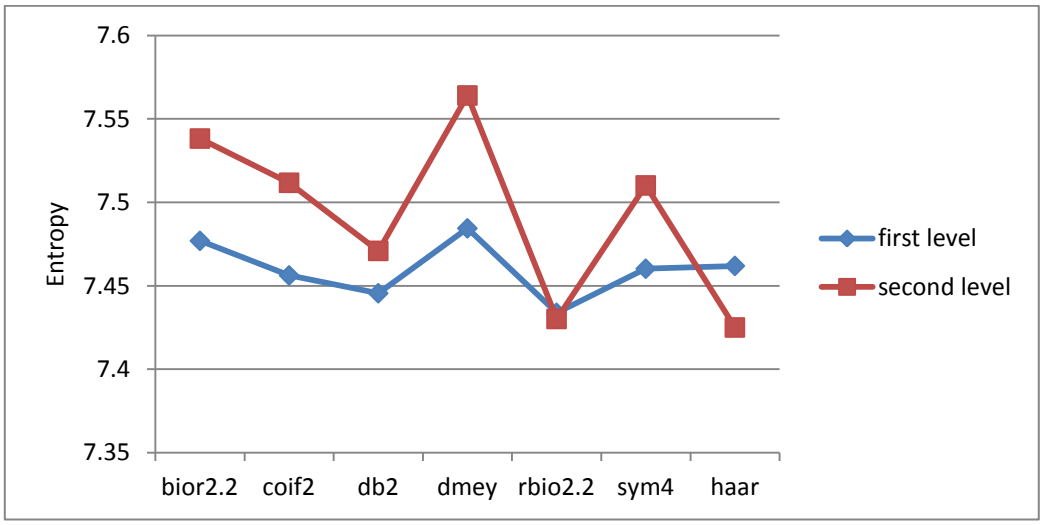

Fig4.48 Variation of Entropy for different wavelets at first and second decomposition level for image1

Figure(4.49)shows the Entropy values for the value of results obtained from the second case in the first and second levels from different waves in bior2.2, coif2, db2, dmey, rbio2.2, sym4, and haar. It was clearly noted that Entropy results were better at the second level in the first level.

This is due to the level of decomposition used to transform the wavelets, Increased depth of analysis leads to better results in most types of wavelets used for detection of tumor .

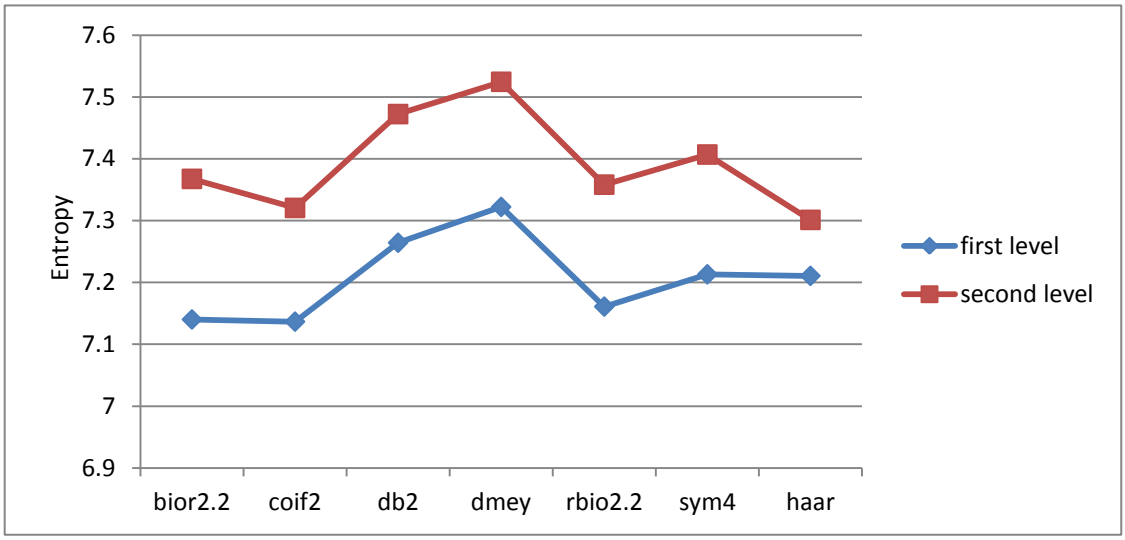

Fig4.49 Variation of Entropy for different wavelets at first and second decomposition level for image2

Figure (4.50)shows the Entropy values for the value of results obtained from the third case in the first and second levels from different waves in bior2.2, coif2, db2, dmey, rbio2.2, sym4, and haar. It was clearly noted that Entropy results were better at the second level. This is due to the level of decomposition used to transform the wavelets, Increased depth of analysis leads to better results in most types of wavelets used for detection of tumor .

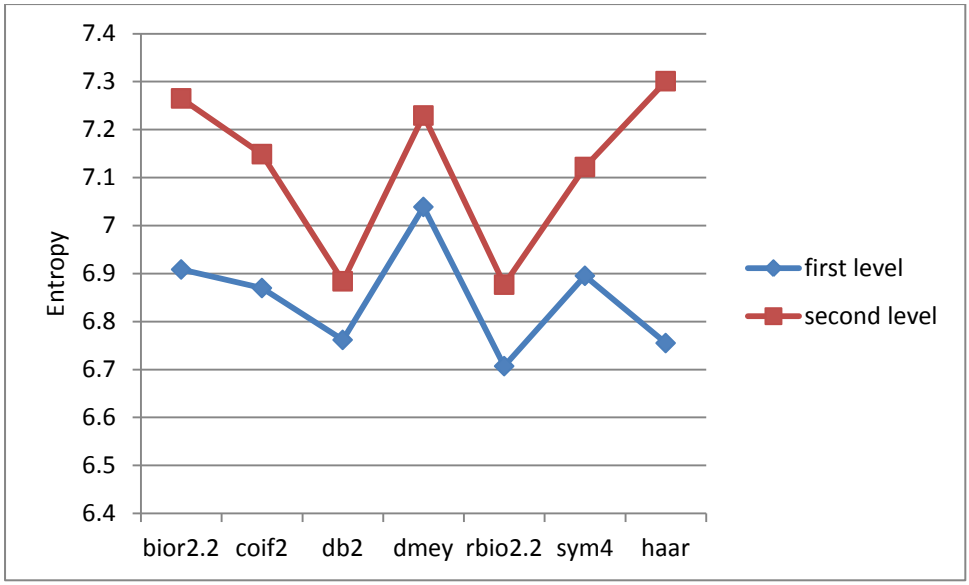

Fig4.50 Variation of Entropy for different wavelets at first and second decomposition level for image3

Figure(4.51) shows the Entropy values for the results value obtained from the fourth case in the first and second levels from different waves in bior2.2, coif2, db2, dmey, rbio2.2, sym4 and haar. It was clearly noted that Entropy results were better at the second level. This is due to the level of decomposition used to transform the wavelets, Increased depth of analysis leads to better results in most types of wavelets used for detection of tumor .

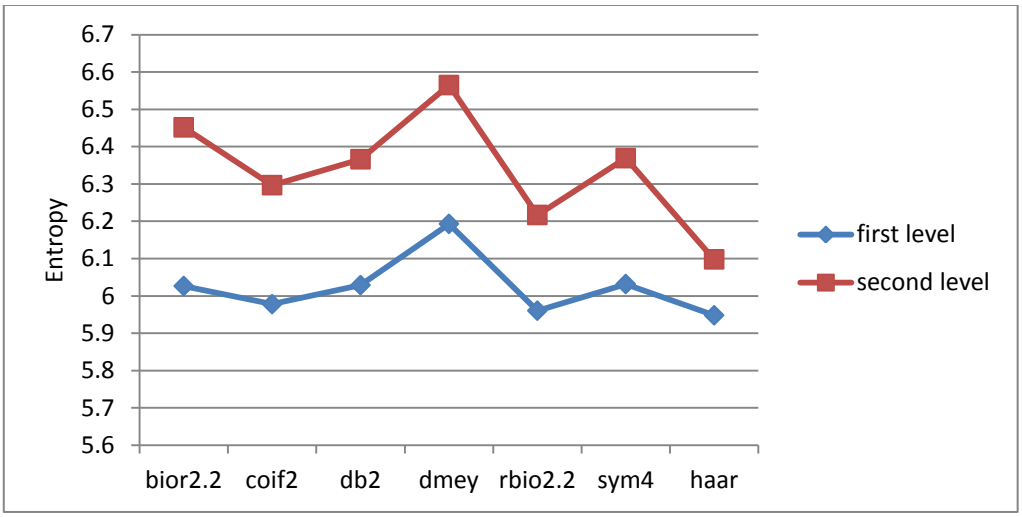

Fig4.51 Variation of Entropy for different wavelets at first and second decomposition level for image4

Figure (4.52) shows the Entropy values for the results value obtained from the fourth case in the first and second levels from different waves in bior2.2, coif2, db2, dmey, rbio2.2, sym4 and haar. It was clearly noted that Entropy results were better at the second level. This is due to the level of decomposition used to transform the wavelets, Increased depth of analysis leads to better results in most types of wavelets used for detection of tumor .

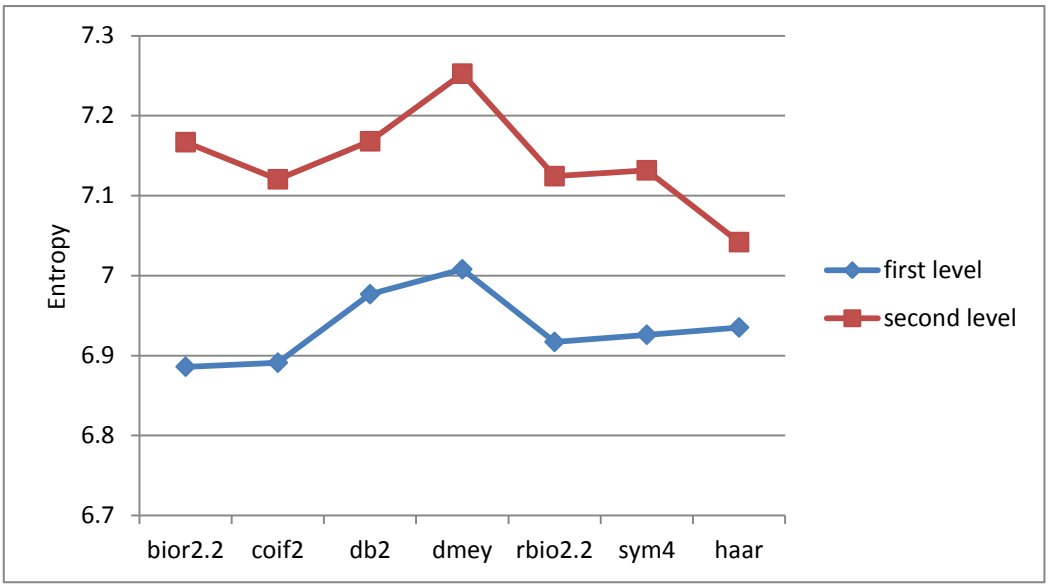

Fig4.52 Variation of Entropy for different wavelets at first and second decomposition level for image5

4.7 General notes

from the previous results we can conclude the following:

1- A distinction was made between the infected and the uninfected images, as it becomes clear to us that the images 1, 2 and 3 have a brain tumor. Images 4 and 5 had not by a tumor.

2- The higher the number of decomposition levels of wavelet decay, the better results. Except for Rbio2.2 waves are better at first decomposition level

3- It can be seen that haar wavelet performance is better with PSNR at the first and second level for tumor detection.

4- The dmy wavelets have given the best results with Entropy at the first and second level for tumor detection.
5- The introduced approach has gaven the better result than the technique uses in the 'Wavelet Based Image Fusion for Detection of Brain Tumor'[7].According to the values of
PSNR for image 1.

CHAPTER FIVE
Conclusion and Future Scope

5.1 Conclusions

Brain cancer has attracted the attention of researchers to implement different technologies in the detection process. Wavelet transform is one of technologies employed for brain tumors detection. This thesis proposed new method for Brain tumor detection. It merges multi-focus images using discrete wavelet transform (DWT). MRI and CT grey images were merged by taking a the maximum absolute value from symmetric pixels. And then the merged image is inverted to reconstruct the image (IDWT). As result, the obtained images was improved which improve the brain tumor detection as well. The higher number of decomposition levels the best resulting in PSNR and Entropy for tumor detection. While in rbio 2.2 gives better results in the first level. However, the best results was obtained from haar, db2 and coif1 with PSNR. The wavelet dmy was gave the best results with Entropy.

5.2 Future work

The following steps can be taken as recommendations for future works:

- Pictures can be combined using different wavelengths at more than two levels on different wavelets and results can be compared.
- The combine more than two medical images, for example combining CT images, MRI images and Single Photon Emission Computed Tomography (SPECT) scans can make medical diagnosis easier and more accurate better tumor detection .
- The Python program can be applying instead of the Matlab program to follow same technique for Brain tumor detection by multi -focus image fusion based on wavelet transform.

REFERENCES

REFERENCES

[1] Singh, S. K., Clarke, I. D., Terasaki, M., Bonn, V. E., Hawkins, C., Squire, J., & Dirks, P. B. (2003). Identification of a Cancer Stem Cell in Human Brain Tumors Identification of a Cancer Stem Cell in Human Brain Tumors. *Cancer Research*, (63), 5821–5828.

[2] M. B. Cuadra, C. Pollo, A. Bardera, O. Cuisenaire, J. G.Villemure, and J. P. Thiran, "Atlas- based segmentation of pathological MR brain images using a model of lesion growth.

[3] Manpreet Kaur, Dr. Shiv Kumar Verma and Gagandeep Kaur," Medical image fusion using wavelet transform", International Journal For Technological Research In Engineering ,Volume 2, Issue 11, July-2015,pp.2525-2528.

[4] Rajiv Singh and Ashish Khare," Multiscale Medical Image Fusion in Wavelet Domain", The ScientificWorld Journal, 2013,pp.1-10.

[5] Hill, Paul R., Cedric Nishan Canagarajah, and David R. Bull. "Image Fusion Using Complex Wavelets." *BMVC*. 2002.

[6] Sapkal, R. J., and S. M. Kulkarni. "Image fusion based on wavelet transform formedical application." International Journal of Engineering Research and Applications 2.5 (2012): 624-627.

[7] Dwith, C. Y. N., Vivek Angoth, and Amarjot Singh. "Wavelet based image fusion for detection of brain tumor." International Journal of Image, Graphics and Signal Processing 5.1 (2013): 25.

[8] Haribabu, Maruturi, CH Hima Bindu, and K. Satya Prasad. "A New Approach of Medical Image Fusion using Discrete Wavelet Transform." International Journal on Signal and Image Processing 4.2 (2013): 21.

[9] Sentamilselvan, R., and M. Manikandan. "Discrete Wavelet Transform Based Brain Tumor Detection using Haar Algorithm." International Journal of Data Mining Techniques and Applications 5.1 (2016): 83-86.

[10] Vaishnavi, D. S. R. G., and S. Mehekare. "Detection of Brain Tumor Using Discrete Wavelet Transform PCA & KSVM." International Journal of Innovative Research in Computer and Communication Engineering (IJIRCCE) 5 (2017): 10228-10236.

[11] jany Shabu, S. L., and C. Jayakumar. "Multimodal image fusion using an evolutionary based algorithm for brain tumor detection." (2018).

[12] Patil, Anjali, and M. N. Tibdewal. "Wavelet Transform Based Medical Image Fusion with Different Fusion Methods." Journal of Engineering Research and Application 5.3:10-14.

[13] Thakral, Shaveta, and Pratima Manhas. "Image processing by using different types of discrete wavelet transform." International Conference on Advanced Informatics for Computing Research. Springer, Singapore, 2018.

[14] Pandey, Atul Kumar. "Analysis of Robotic Systems Using Haar Wavelet." (2018).

[15] Monica, A., D. Devarajan, and L. Ramachandran. "Diffusion Tensor MRI of Human Heart using Wavelet Based Approach."

[16] Kumar, S. Suresh, and H. Mangalam. "Wavelet-based Image Compression of Quasi Encrypted Grayscale Images." International Journal of Computer Applications 45 (2012).

[17] Tammireddy, Prahallada Reddy, and Rajesh Tammu. "Image Reconstruction using wavelet transform with extended fractional fourier Transform." (2014).

[18] Babu, G., and R. Sivakumar. "Comparative Analysis of MRI-PET Brain Image Fusion and Using Discrete Wavelet Transform" Proceedings of the International Conference on Graphics Signal *Processing*. 2017.

[19] Váňa, Zdeněk. "Discrete Wavelet Transform in Linear System Identification."Fusion Using Discrete Wavelet Transform" Proceedings of the International 2014.

[20] Mishra, Hari Om Shanker, and Smriti Bhatnagar. "MRI and CT image fusion based on wavelet transform." International Journal of Information and ComputationTechnology 4.1 (2014): 47-52.

[21] Soman, K. P., and K. I. Ramachandran. Insight Into Wavelets From Theory To Practice 2Nd Ed. PHI Learning Pvt. Ltd., 2005.

[22] Angoth, Vivek, C. Y. N. Dwith, and Amarjot Singh. "A novel wavelet based image fusion for brain tumor detection." International Journal of computer vision and signal processing 2.1 (2013): 1-7.

[23] Sahu, Vinay, and Dinesh Sahu. "Image Fusion using Wavelet Transform: A Review." Global Journal of Computer Science and Technology (2014).

[24] Parmar, Kiran, Rahul K. Kher, and Falgun N. Thakkar. "Analysis of CT and MRI on image fusion using wavelet transform." 2012 International Conference Communication Systems and Network Technologies. IEEE, 2012.

[25]https://shodhganga.inflibnet.ac.in/bitstream/10603/197980/13/13_chapter-4.pdfm

[26] Wakure, S., and S. Todmal. "Survey on different image fusion techniques." IOSR J VLSI Signal Process 1.6 (2013): 42-48.

[27] G. Kaur and P. Kaur. Survey on multifocus image fusion techniques. International Conference on Electrical, Electronics, and Optimization Techniques (ICEEOT). pp.1420- 1425, 2016.

[28] Ambily, P. K., Shine P. James, and Remya R. Mohan. "Brain Tumor Detection using Image Fusion and Neural Network." International Journal of Engineering Research and General Science 3.2 (2015).

[29] Wahyuni, Ias Sri. Multi-focus image fusion using local variability. Diss. 2018.

[30] Angoth, Vivek, C. Y. N. Dwith, and Amarjot Singh. "A novel wavelet based image fusion for brain tumor detection." International Journal of computer vision and signal processing 2.1 (2013): 1-7.

[31] Mane, Sonali, and S. D. Sawant. "Image Fusion On Mr And Ct Images Using Wavelet Transforms And Dsp Processor." International Journal of Engineering Trends and Technology (IJETT) Vol 4.

[32] Gurusamy, Vairaprakash, S. Kannan, and G. Nalini. "REVIEW ON IMAGE SEGMENTATION TECHNIQUES."

[33] Kaur, Dilpreet, and Yadwinder Kaur. "Various image segmentation techniques: a review." *International Journal of Computer Science and Mobile Computing* 3.5 (2014): 809-814.

APPENDIX

MATLAB Code for 1-Level Wavelet Image Fusion:

```
        close all;clear% clear previous run data and figures
%List of Wavelet types
wtype={'bior2.2','coif1','db2','dmey','rbio2.2','sym4','haar
'}
%List of MRI and CT test images
x1={'mr1.jpg','mr_2.jpg','mr_33.jpg','mr_5.jpg','mr_7.jpg'}
 x2={'ct1.jpg','ct_2.jpg','ct_33.jpg','ct_5.jpg','ct_7.jpg'}
% there are two loops first for test images (cases) and the
second is for
% wavelet types
for i=1:5
%% Read Images
% the size of images must be equal and resized to 128x28
a=imread(x1{i});
a=imresize(a,[128 128]);
b=imread(x2{i});
b=imresize(b,[128 128]);
for j=1:7
% recall the wavelet type
    wave_type=wtype{j};
%%   Wavelet Transform for  MRI and CT images
[a1,b1,c1,d1]=dwt2(a,wave_type);
[a2,b2,c2,d2]=dwt2(b,wave_type);
[k1,k2]=size(a1);
%% Fusion Rules where the maximum values are taken from
wavelet MRI and CT images

        a3=max(a1,a2);
        b3=max(b1,b2);
        c3=max(c1,c2);
        d3=max(d1,d2);

%% Inverse Wavelet Transform of fused image
c=idwt2(a3,b3,c3,d3,wave_type);

%% Performance Criteria: calculation of RMSE, PSNR, and
Entropy for each case
% and with different wavelet types
E=mean(sqrt(sum(sum((double(a)-double(c)).^2))/(128*128)))
PSNR(i,j)=20*log10(256/E)
Entropy(i,j)=entropy(rgb2gray(uint8(c)))
end
%Display the results: MRI and CT image and Fused Image
figure
subplot(1,3,1),imshow(a)
title('MRI Image')
subplot(1,3,2),imshow(b)
title('CT Image')
subplot(1,3,3),imshow(uint8(c),[])
```

```
title('Fused Image')
end
% Save PSNR and Entropy to compared with Wavelet 2-Levels
and Segmantation
save('psnrL1','PSNR')
save('Entropy1','Entropy')
```

MATLAB Code for 2-Level Wavelet Image Fusion:

```
close all;clear% clear previous run data and figures
%List of Wavelet types
wtype={'bior2.2','coif1','db2','dmey','rbio2.2','sym4','haar'}
%List of MRI and CT test images
x1={'mr1.jpg','mr_2.jpg','mr_33.jpg','mr_5.jpg','mr_7.jpg'}
x2={'ct1.jpg','ct_2.jpg','ct_33.jpg','ct_5.jpg','ct_7.jpg'}
% there are two loops first for test images (cases) and the
second is for
% wavelet types
for i=1:5
%% Read Images
% the size of images must be equal and resized to 128x28
a=imread(x1{i});
a=imresize(a,[128 128]);
b=imread(x2{i});
b=imresize(b,[128 128]);
for j=1:7
% recall the wavelet type
    wave_type=wtype{j};
%% Level 1  Wavelet Transform for MRI and CT images
[a1,b1,c1,d1]=dwt2(a,wave_type);
[a2,b2,c2,d2]=dwt2(b,wave_type);
%% Level 2  Wavelet Transform for MRI and CT images
[aa1,bb1,cc1,dd1]=dwt2(a1,wave_type);
[aa2,bb2,cc2,dd2]=dwt2(a2,wave_type);
[k1,k2]=size(a1);
%% Fusion Rules where the maximum values are taken from
wavelet MRI and CT images
% Fusion process is applied on Level1 and Level2

        a3=max(a1,a2);
        b3=max(b1,b2);
        c3=max(c1,c2);
        d3=max(d1,d2);
        aa3=max(aa1,aa2);
        bb3=max(bb1,bb2);
        cc3=max(cc1,cc2);
        dd3=max(dd1,dd2);
%% Level2 Inverse Wavelet Transform  of fused image
cc=idwt2(aa3,bb3,cc3,dd3,wave_type);
%% Level1 Inverse Wavelet Transform
c=idwt2(cc(1:size(a3,1),1:size(a3,2),:),b3,c3,d3,wave_type);
```

```
%% Performance Criteria: calculation of RMSE, PSNR, and
Entropy for each case
% and with different wavelet types
E=mean(sqrt(sum(sum((double(a)-double(c)).^2))/(128*128)))
PSNR2(i,j)=20*log10(256/E)
Entropy2(i,j)=entropy(rgb2gray(uint8(c)))
end
%Display the results: MRI and CT image and Fused Image
figure
subplot(1,3,1),imshow(a)
title('MRI Image')
subplot(1,3,2),imshow(b)
title('CT Image')
subplot(1,3,3),imshow(uint8(c),[])
title('Fused Image')
end
% Save PSNR and Entropy to compared with Wavelet 1-Level and
Segmantation
save('psnrL2','PSNR2')
save('Entropy2','Entropy2')
```

MATLAB Code for MRI Image Segmentation:

```
clear,close all% clear previous run data and figures
In='mr1.jpg';%test image file
%++++++++++++++++++++++++++++++++++++++++++++++++++++++++++++
+++
%% % Read Input Image
s0=(imread(In));
%Resize input image to 128x28
s0=imresize(s0,[128 128]);
s=s0;
figure;
%Display input image
imshow(s);
title('Input image','FontSize',20);
%% Filter
% Filter Parameters
num_iter = 10;
    delta_t = 1/7;
    kappa = 15;
    option = 2;
    disp('Preprocessing image please wait . . .');
    %Filtering Image using Finite differences and
Convolution
    inp = anisodiff(s,num_iter,delta_t,kappa,option);
    inp = uint8(inp);
    %Resize resulting image to 128x28 and if it is colored
convert to gray-level
inp=imresize(inp,[128,128]);
if size(inp,3)>1
    inp=rgb2gray(inp);
```

```
end
%Display filtered image

figure;
imshow(inp);
title('Filtered image','FontSize',20);
%% thresholding
% convert to binary image where pixels > threshold are set
to 1
%otherwise set to 0
sout=imresize(inp,[128,128]);
t0=60;%;
th=t0+((max(inp(:))+min(inp(:)))./2);
for i=1:1:size(inp,1)
    for j=1:1:size(inp,2)
        if inp(i,j)>th
            sout(i,j)=1;
        else
            sout(i,j)=0;
        end
    end
end
%% Morphological Operation
label=bwlabel(sout);%Label connected components in 2-D
binary image
stats=regionprops(logical(sout),'Solidity','Area','BoundingB
ox');%Measure properties of image regions
density=[stats.Solidity];%Rigions density
area=[stats.Area];%Rigions area
high_dense_area=density>0.7;%assume high dense area is > .7
max_area=max(area(high_dense_area));%find maximum high dense
area
%tumor area is considered as largest area
tumor_label=find(area==max_area);
tumor=ismember(label,tumor_label);
%tumor assumed to have area > 100 pixels
if max_area>100%50
    %Display tumor area
   figure;
   imshow(tumor)
   title('tumor alone','FontSize',20);
else
    % the object is not tumor if its area <= 100 pixels
    h = msgbox('No Tumor!!','status');
    return;
end

%% Bounding box
%Bounding Box is The smallest rectangle containing the
region and
%reprsented by four values x y w h
```

```
%x is x coordinates of box starting point
%y is y coordinates of box starting point
%w and h are width and hieght of the bounding box
box = stats(tumor_label);
wantedBox = box.BoundingBox;
figure
%Display filtered image
imshow(inp);
title('Bounding Box','FontSize',20);
hold on;
%Display the bounding box
rectangle('Position',wantedBox,'EdgeColor','y');
hold off;
%% Getting Tumor Outline - image filling, eroding,
subtracting
% erosion the walls by a few pixels
dilationAmount = 5;
rad = floor(dilationAmount);
[r,c] = size(tumor);
filledImage = imfill(tumor, 'holes');
for i=1:r
   for j=1:c
       x1=i-rad;x2=i+rad;y1=j-rad;y2=j+rad;
       if x1<1,x1=1;end
       if x2>r,x2=r;end
       if y1<1,y1=1;end
       if y2>c,y2=c;end
       erodedImage(i,j) =
min(min(filledImage(x1:x2,y1:y2)));
   end
end
figure
%Display eroded image
imshow(erodedImage);
title('eroded image','FontSize',20);
%% subtracting eroded image from original BW image
tumorOutline=tumor;
tumorOutline(erodedImage)=0;
figure;
imshow(tumorOutline);
title('Tumor Outline','FontSize',20);
%% Inserting the outline in filtered image in green color
rgb = inp(:,:,[1 1 1]);
red = rgb(:,:,1);
red(tumorOutline)=255;
green = rgb(:,:,2);
green(tumorOutline)=0;
blue = rgb(:,:,3);
blue(tumorOutline)=0;
tumorOutlineInserted(:,:,1) = red;
tumorOutlineInserted(:,:,2) = green;
```

```
tumorOutlineInserted(:,:,3) = blue;
figure
imshow(tumorOutlineInserted);
title('Detected Tumer','FontSize',20);
%% Display All results
figure
subplot(231);imshow(s);title('Input image','FontSize',20);
subplot(232);imshow(inp);title('Filtered
image','FontSize',20);
subplot(233);imshow(inp);title('Bounding
Box','FontSize',20);
hold on;rectangle('Position',wantedBox,'EdgeColor','y');hold
off;
subplot(234);imshow(tumor);title('tumor
alone','FontSize',20);
subplot(235);imshow(tumorOutline);title('Tumor
Outline','FontSize',20);
subplot(236);imshow(tumorOutlineInserted);title('Detected
Tumor','FontSize',20);
%++++++++++++++++++++++++++++++++++++++++++++++++++++++++++++++
+++
%% Display the segmented  tumor area
a1=wantedBox(1);
b1=wantedBox(2);
a2=wantedBox(1)+wantedBox(3);
b2=wantedBox(2)+wantedBox(4);
t1=inp(b1(1):b2(1),a1(1):a2(1));
t22=rgb2gray(imread('mr1.jpg'));
[MM2,NN2]=size(t22);
 t2=t22(MM2/2+1:end,1:NN2/2);%case 1,3
 imshow(t1);title('segmented tumor area','FontSize',20)
 %% Performance Criteria: calculation of RMSE, PSNR, and
Entropy
[MM1,NN1,~]=size(t1);
[MM2,NN2,~]=size(t2);
mm=min(MM1,MM2);nn=min(NN1,NN2);
MSE=sum(sum((double(t1(1:mm,1:nn))-
double(t2(1:mm,1:nn))).^2))/(mm*nn);
PSNR=mean(10*log10(256^2/MSE))
Entropy=entropy(rgb2gray(uint8(ti)))
```